13. Climate change scenarios for the Italian mountains

Gualdi S.[1], Cavicchia L.[1], Scoccimarro E.[1], Reder A.[1], Barbato G. [1], Montesarchio M. [1], Raffa M. [1], Mercogliano P.[1], Dell'Aquila A.[2], Artale V.[2]

[1]*Euro Mediterranean Center on Climate Change (CMCC), Italy*
[2]*ENEA, Rome, Italy*

Global warming is impacting mountain regions in a particularly severe way, posing a very serious threat to the environment of these areas. Over the last decades, global warming has caused most of (if not all of) Alpine glaciers to recede, affecting discharge of alpine rivers and increasing natural hazards. Future climate change is projected to exacerbate further these trends. The water regime of the Italian mountain areas is projected to undergo substantial changes and because the Alps are the primary source for such major rivers as the Po, Rhine, Danube, Rhone, the impact of a changed mountain climate, and in particular of the precipitation regimes, will be felt far beyond mountainous regions themselves.

Reliable estimates of future climate change in the Alpine region are relevant for large parts of the European society and particularly for the Italian one. At the same time, the complex Alpine region poses considerable challenges to climate models, which translate to uncertainties in the climate projections.

In the framework of the NextData project, numerous simulations were collected and conducted and then analyzed, in order to produce an estimate, as reliable as possible, of the signal of climate change that could occur in the next decades in the Alpine region, and in the Italian mountains, as a consequence of future emission scenarios. For this purpose, simulations obtained from global and regional, coupled ocean–atmosphere and atmospheric only models, at different spatial resolutions have been considered and analyzed. As a first step, analyses of the capability of models to reproduce the main features of the observed climate (including extreme events) have been conducted, then the climate change signal provided by the models' simulations has been evaluated.

This Chapter provides a summary of the main results obtained from these analyses, where the climate change signals detectable both in the mean values, variability and extreme events over the Mediterranean area, Italian Peninsula and especially Alpine region are illustrated and discussed.

In Section 13.1, the main features of observed climate variability and weather extremes at regional scale, and the capability of numerical models to simulate them, are considered and discussed. Section 13.2 provides an overview of the climate change signal at global scale and for the Mediterranean basin, whereas Section 13.3 illustrates the expected changes projected for the Italian mountain areas.

13.1 Climate variability and weather extremes in the Euro–Mediterranean region

In this section, numerical simulations of climate variability and extreme events in the Euro–Mediterranean region are considered and discussed to provide an overview of models' ability to

reproduce these important climatic features, and present how extreme events are projected to change at the end of the century.

13.1.1 Regional Climate simulations of the Mediterranean climate low–frequency variability

In a recent study, Dell'Aquila et al. (2018) considered a sub–set of the Med-CORDEX simulations (for more details, see Dell'Aquila et al., 2018) over the period 1979-2011 to evaluate the models' capability to represent observed decadal variations over the Euro-Mediterranean region. The Med–CORDEX simulations have been analysed and compared with different observational and re–analysis data sets (e.g., ERA–Interim Dee et al., 2011; CRU, Harris et al., 2013). This kind of analysis and comparison are needed to provide an evaluation of the model's performance, useful to future model development and to inform potential user of the simulations about model's ability to provide a reliable estimate of climate variability and climate change signals and related uncertainties.
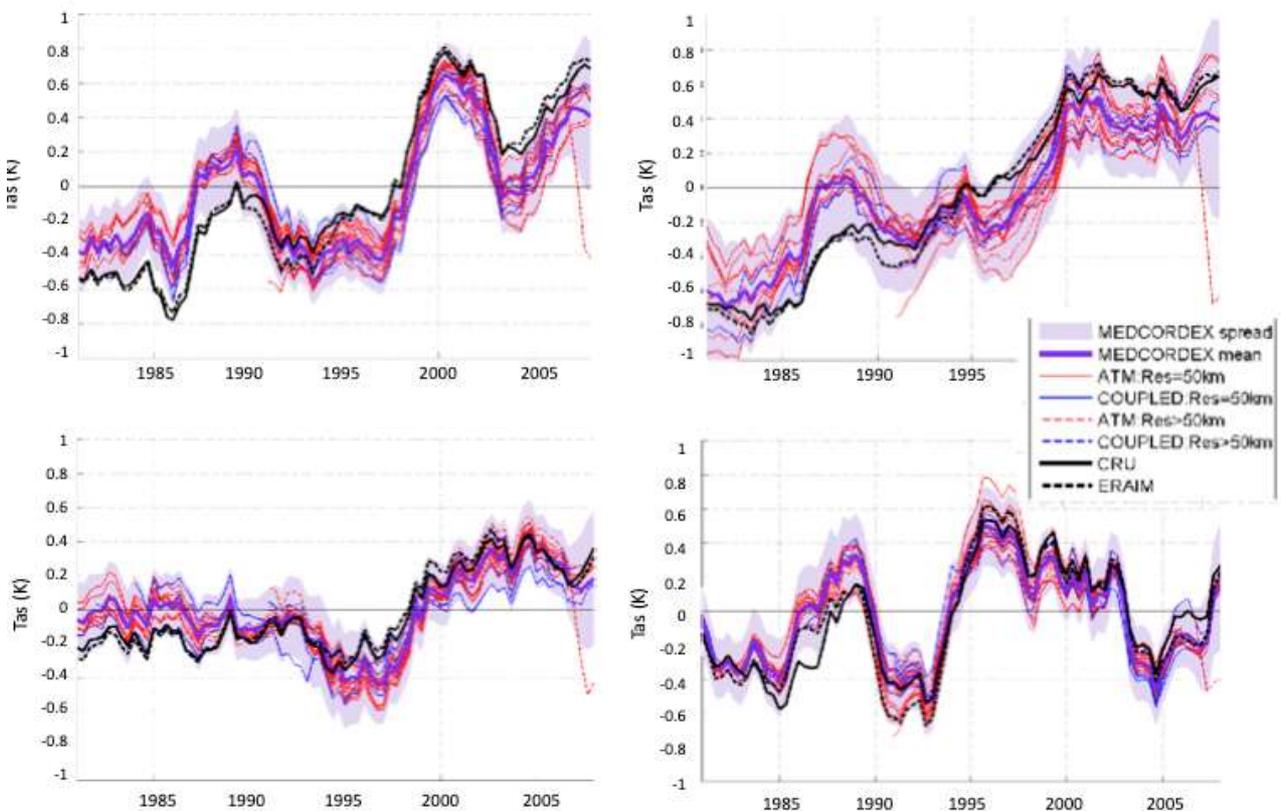

Figure 1. *Observed and Med-CORDEX simulated decadal climate anomalies in the Mediterranean region (see black box in Figure 1) over the period 1979–2011. We show the surface air temperature anomalies (Tas, land-only; K); from CRU, ERA-Interim and Med-CORDEX simulations (legend on the right) for different seasons. The red solid lines are for stand-alone atmospheric simulations with a resolution of 50 km (Med-44; Med-44i), blue lines are for the coupled systems. The dashed lines are for runs with resolution higher than 50 km (i.e. Med-22, Med-18, Med-11). The thick purple line is for the Med-CORDEX multi-model ensemble mean, and the shaded areas depict the multi-model spread (+/- 1 standard deviation). Mean anomalies relative to 1979–2011 with a 5-year running mean are shown.*

The skill of Med-CORDEX regional climate simulations has been evaluated in terms of their capability to reproduce the basic features of observed multi–annual to decadal changes for some of the most

common variables used for impact studies, such as near–surface air temperature and precipitation over the Euro-Mediterranean region.

An interesting feature of Med–CORDEX simulations is that they include a variety of different RCM configurations, i.e. atmospheric stand–alone models, ocean–atmosphere coupled models, implemented with a wide range of horizontal resolutions, from ~50 to ~12 km. Despite the quite substantial differences in the model set–ups, results do not show evident differences in the capability of the models to reproduce the multi–year to decadal temperature anomalies (Figure 1). Albeit, with some notable exceptions, all of the considered Med–CORDEX models generally capture the relatively warmer and cooler periods over a Mediterranean box (only land points; LON: 10W-40E; LAT: 30N-48N). However, when compared to both CRU and ERA–Interim, the amplitude of the simulated anomalies shows errors up to 0.5 K (not shown), for all considered seasons. In particular, the Med–CORDEX runs exhibit a warm bias in late 1980s, especially during boreal spring (MAM) and summer (JJA), followed by anomalies that are generally smaller than observed after 1995. This bias, common to basically all of the Med–CORDEX simulations, leads to a general underestimation of the observed trend in near–surface temperature, especially in the summer and spring seasons (Dell'Aquila et al., 2018).
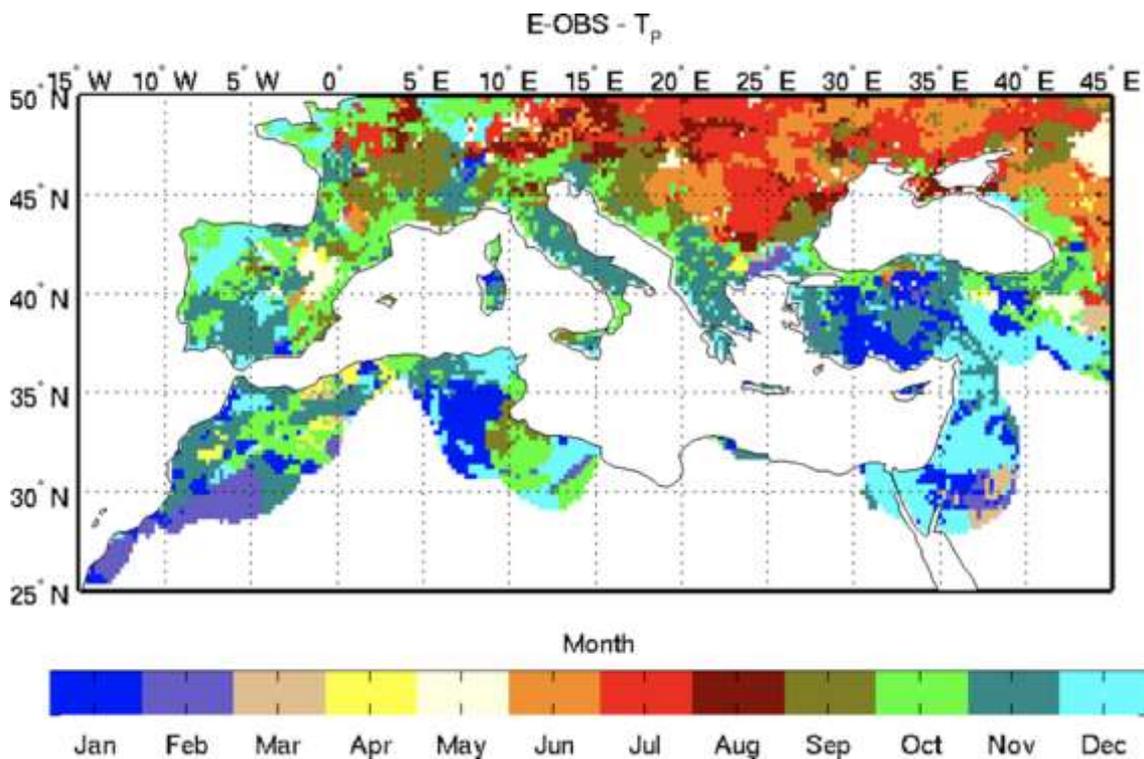

Figure 2. Timing of extreme precipitation events in E-OBS dataset (version 11.0, Haylock et al. 2008). Areas where E-OBS has no data are represented as white. Picture from Cavicchia et al. (2018).

So far, we have discussed the ability of regional climate models specifically designed to simulate the climate variability and change in the Euro–Mediterranean region, showing that, despite some (relatively small) systematic errors, they are reasonably able in reproducing the low–frequency variations of the climate in the target region. Now, in the following, we will consider and discuss the ability of climate models to simulate extreme events and how the characteristics of these events in the target region might be possibly affected by global warming.

13.1.2 Regional Climate simulations of extreme events in the Euro–Mediterranean area

Exploiting the added value of the Med–CORDEX models' ensemble, including several very high resolution and/or coupled simulations, Cavicchia et al. (2018) performed a comparison of the skill of different reanalysis and modelling datasets in reproducing the observed features of Mediterranean extreme precipitation events. In their analysis, the characterisation of extreme precipitation statistics is based on the 99th percentile (P99) of the wet day precipitation intensity probability distribution function. Moreover, the agreement between observed and modelled extreme precipitation has been assessed by performing a statistical test taking into account the tails of the precipitation intensity distributions.

The Cavicchia et al. (2018) analysis effort provided two main achievements. First, a novel approach for the sub–setting of the domain based on the timing of precipitation (i.e. the maximum in the twelve months histogram of events exceeding the precipitation 99th percentile) has been provided (Figure 2).
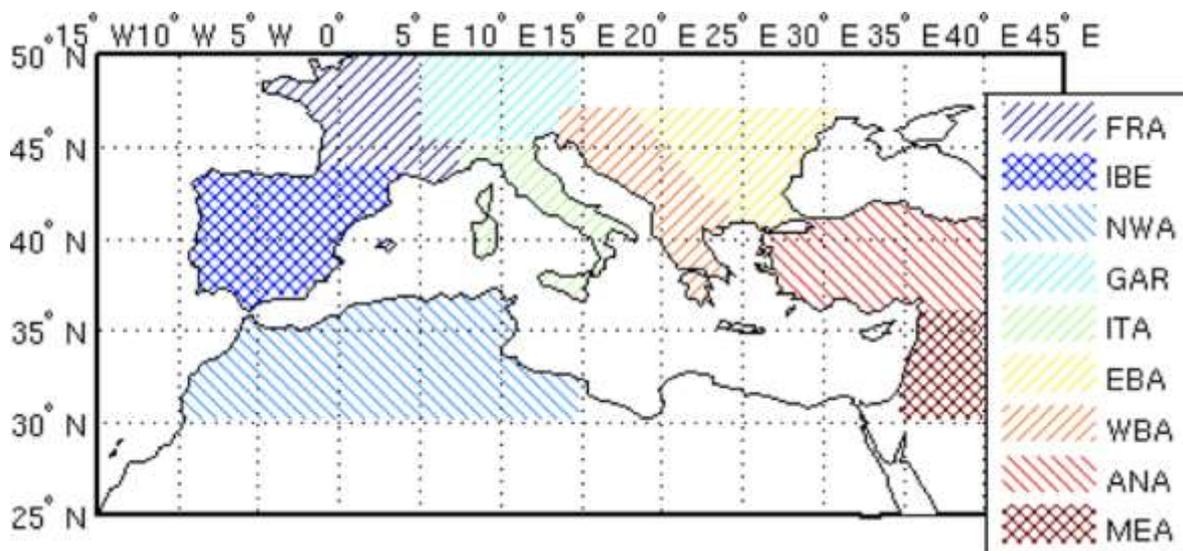

Figure 3. Sub-regions used in the analysis: France (FRA), Iberia (IBE), north-west Africa (NWA), great Alpine region (GAR), Italy (ITA), eastern Balkans (EBA), western Balkans (WBA), Anatolia (ANA), Middle East (MEA).

Such approach allows to divide the domain in several sub–regions by clustering areas characterised by coherent timing behaviours. The resulting areas (Figure 3 and see Cavicchia et al., 2018 for more details) are thus defined in a way that relies on the physical properties of precipitation rather than on merely geographical criteria, providing a more meaningful insight on the typical variability patterns of the considered diagnostics.

Model inter-comparison for the variable P99 is shown in Figure 4, in terms of Taylor diagrams. Considering the correlation with observations, a number of regions emerges, where most of the datasets appear to be more skilled in reproducing the observed patterns: Iberia, France, the great Alpine region and Anatolia. The largest deviations from observation are found, on the other hand, in the eastern Balkans and north-west Africa regions. Moreover, within the same region, the different types of dataset analysed (reanalysis, high/low resolution coupled/uncoupled models) exhibit generally a correlation with observations comparable to each other, independently on the

overall performance in the specific region. In other words, it is found that the skill in reproducing observation exhibits a larger spread between different regions, than between different datasets.

On the other hand, focusing on spatial variability, reanalyses tend on average to show a smaller standard deviation compared to observations, while high-resolution models show standard deviation generally larger than observations. The spatial variability values found in low resolution models are equally distributed below and above the one of reference observation dataset. Such behaviour can be explained in part as an effect of varying resolution of different datasets (interpolation and averaging process).

However, reanalysis datasets, even though they have comparable resolution with the coarser resolution models, tend to exhibit smaller values of spatial variability.

Concerning the root mean square error, in regions where the patterns are better reproduced (France, Iberia, great Alpine region) most of the models show a comparable error, while the RMSE range spanned by different models increases proportionally to the decrease in spatial correlation.

Finally, Cavicchia et al. (2018) found that for models for which paired coupled–uncoupled runs are available, the two simulations produce generally values of both correlation and spatial variability very close to each other. So, the skill of these models in reproducing extreme precipitation events does not appear to be substantially affected by air–sea coupling.
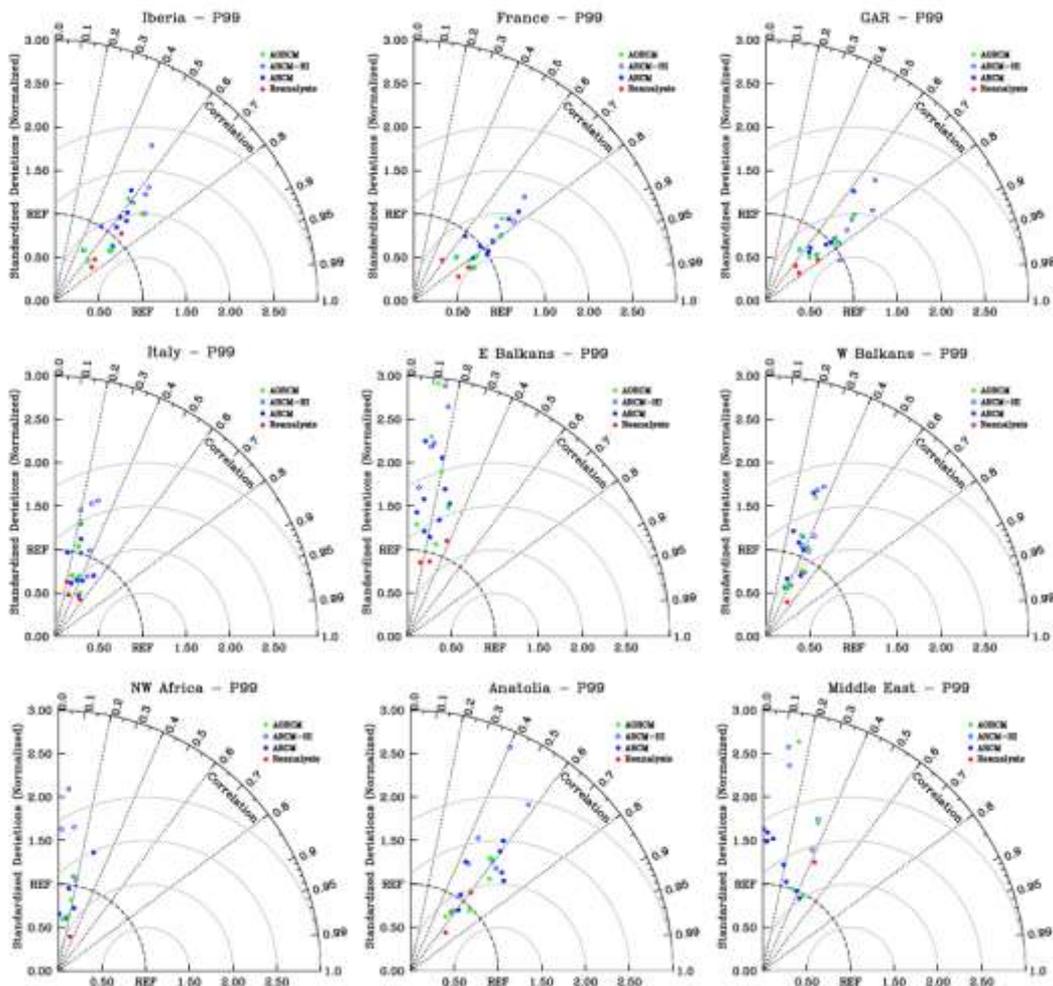

Figure 4. Taylor plots of 99th percentile of daily precipitation in different datasets, for the nine sub-regions as indicated in the title bar of each panel. Red dots reanalysis datasets; blue dots atmosphere-only RCMs; blue circles high resolution

In order to investigate the dependence on the analysed sub–region of the skill in reproducing the observed statistics of extreme precipitation events exhibited by the different datasets in a coherent way, Cavicchia et al. (2018) took into account the contributions to the extreme precipitation events from large scale and convective precipitation. Results (not shown) indicate that the regions where the modelled extreme precipitation is in better agreement with the observations (Iberia, great Alpine region, Anatolia, France: see Figure 4) are the ones where large–scale precipitation gives a significant contribution to extreme precipitation. Similar results are found for the CMCC model (not shown). Such behaviour has been observed also in previous studies based on global models (Iorio et al., 2004; Kopparla et al., 2013).

Finally, to shed further light on the possible dependence on model configurations of the skill in reproducing the observed statistics of extreme precipitation events, several realisations of the hindcast simulation performed with one specific model (the CMCC model) implemented in different configurations have been analysed. The results suggest that increasing resolution and switching on the coupling has a mild impact on the long–term statistics of extreme precipitation. Changes of the convective parameterisation on the other hand, turn out to have a relatively larger impact on the correlation of the analysed diagnostics quantities with observations. The effect of physical parameterisations is particularly relevant in areas where extreme precipitation events are dominated by convective rather than large-scale precipitation, consistently with the sub–setting described above. Importantly, as model resolution keeps increasing, along with their ability in representing heavy precipitation processes, the necessity of observational datasets of high quality and comparable resolution emerges.

13.2 Expected climate change at global and regional scales

The Earth's climate is changing, as now numerous observational evidences are unequivocally demonstrating, and in particular, it is heating up. Warming brought planet's surface temperature to be, on average, almost 1°C warmer than it was in the nineteenth century, with a warming trend that has become particularly intense in the last decades of the twentieth century (IPCC 2013; IPCC 2018). These changes do not only happen for the average temperature values, but other parameters (for example precipitation) and other statistical properties (for example intense and extreme events) start to show signs of alteration (e.g. Scoccimarro et al., 2015; Zampieri et al., 2016).

Concurrent results from a variety of data analyses and numerical experiments have led to the conclusion that global warming observed in the second half of the twentieth century cannot be explained unless anthropogenic forcing is considered (IPCC, 2013). These results and the associated attribution studies have led the scientific community to conclude that a large part of the warming observed in recent decades has been caused by human activities (IPCC, 2013).

Besides, climate change projections indicate that if future human activities will continue to increase atmospheric greenhouse gas emissions at the rate at which they have increased in the recent past, the heating at the end of this century may be on average over 4 °C, but locally this number could also be considerably larger (IPCC, 2013, IPCC 2018). This increase in temperatures could be

accompanied by substantial changes in rainfall, with consequent changes in the distribution of water resources, as well as changes in the statistics of intense and extreme events, highly impacting on our droughts, such as, extreme rainfall, tropical cyclones, droughts, heat waves etc (IPCC, 2013, IPCC, 2018).

13.2.1 Climate change projections over the Euro-Mediterranean region

The Euro-Mediterranean region is generally defined as the area extending over 4000 km in longitude, from the Strait of Gibraltar to the Middle East, and 4000 km in latitude, from Central Europe to North Africa. Over 500 million people, gathered in around 30 states in Africa, Asia and Europe, populate this area.

The complex morphological characteristics and the high environmental vulnerability make this area one of the most interesting case studies from the scientific point of view and relevant from the social point of view.

The Euro-Mediterranean represents a relatively small fraction of the total area of our planet and therefore does not fall within the regions that can determine substantial variations in the global climate. The exception is the role it plays in maintaining the salt equilibrium of the Atlantic Ocean through the inflows and outflows to the Strait of Gibraltar. The Mediterranean Sea itself, a basin almost completely closed and connected to the Atlantic through a strait of just 14.5 Km (Gibraltar), looks like an evaporative basin, with a precipitation deficit estimated at about one meter a year, offset by the relatively low salt water influx of Atlantic water.

Several complex orography systems delimit the region. The Alps, the Atlas and Anatolian mountains and even the most modest, but steep, mountains of the Iberian Peninsula and the Balkans, complicate the dynamic picture. The very presence of the Mediterranean Sea represents another factor of considerable complexity, involving strong thermal gradients and naturally influencing the water cycle of the entire basin.

Regional climate model	ERAIM	CMCC-CM RCP45	CNRM-CM5 RCP45	CNRM-CM5 RCP85	HadGEM2-ES RCP45	HadGEM2-ES RCP85	IPSL-CM5A RCP45	IPSL-CM5A RCP85	MPI-ESM-MR RCP45	MPI-ESM-MR RCP85
CMCC-CCLM				🟧						
CMCC-CCLM421-NEMOMFS										
Med11-CNRM-ALADIN52		🟦								
Med44-CNRM-ALADIN52			🟦	🟧						
Med44I-ENEA-PROTHEUS			🟦							
Med44i-ENEA-RegCM31										
GUF-CCLM4									🟦	🟧
ICTP-RegCM4v.1					🟦					
ICTP-RegCM4.v4										
ICTP-RegCM4.v7							🟧			🟧
IPSL-WRF										
IPSL-WRFNEMOFS										
LMD-LMDZ										
LMD-LMDZNEMOMED							🟦	🟧		
UCLM-PROMES										
UniBelgrade-EBUPOM										

Table 1. *List of Med-CORDEX regional climate projection simulations analysed in this study with corresponding global driver for different RCPs. Specifics about the domains can be found at www.medcordex.eu.*

The overall characteristics of the Mediterranean hydrological cycle and its potential as a source of humidity for central and northern Europe has been investigated by Mariotti et al. (2002a). In this work, among other things, the relationships between the Mediterranean hydrological cycle and large-scale climate variability, especially the NAO, have also been highlighted. In the same year, Mariotti et al. (2002b) showed that precipitation in the Euro-Mediterranean is also linked to the variability of the tropical Pacific (El Niño / Southern Oscillation, ENSO), especially during the autumn and spring seasons.

Besides being strongly affected by climatic variations on a large scale, the Euro–Mediterranean is also characterized by a remarkable variability induced by dynamic mesoscale processes specific for this region, such as for example the orographic cyclogenesis processes and the air-sea interactions that occur in the northern part of the Mediterranean basin (Buzzi and Speranza, 1986; Sanna et al., 2013).

The seasonal cycle is characterized by a strong polarization on the extreme seasons, with rapid and variable transitions. Precipitation is concentrated in the extended winter period (November/March) and summers are generally dry and hot. In the winter period, the dominant circulation is that of the middle latitudes, characterized by the passage of the Atlantic storms; while in the summer period the influences of tropical circulations predominate, with a prevalence of subsidence over the whole area.

The attention to the impacts of global climate change over the highly vulnerable Mediterranean region (e.g. Giorgi 2006; Giorgi and Lionello, 2008) has been increasing over the last few years based on largely consistent projections from several generations of the Coupled Model Intercomparison Project (CMIP) (IPCC, 2007; IPCC, 2013). For example, a recent study by Mariotti et al. (2015) performed using CMIP5 global climate projections has confirmed a tendency for drier and warmer Mediterranean climate in the second half of this century.

The dynamical downscaling approach based on Regional Climate Models (RCMs) has been applied to CMIP3 and CMIP5 global projections with the intent to attain higher resolution and possibly more accurate projections (Feser et al., 2011) at regional scales. For the Mediterranean region, the use of a regionally refined grid is intended to better represent the complex regional orography and associated interactions with the oceanic circulation of the Mediterranean Sea and of the atmosphere above it (Dell' Aquila et al., 2012; Gualdi et al., 2013).

Within the NextData project, regional coupled simulations have been conducted with regional models implemented over the Mediterranean area, in order to produce high–quality data that could provide a better characterization of the climate change signal in the region (e.g. Cavicchia et al., 2018; Dell'Aquila et al., 2018). Furthermore, data obtained from simulations performed in the framework of other international programmes (such as, for example Euro–CORDEX, Jacob et al., 2014, and Med–CORDEX, Ruti et al., 2016) have been collected to explore the low frequency variability over the Mediterranean basin both in terms of weather regimes as well as oceanic circulation.

In the following, the NextData and the Med–CORDEX simulations (see Table 1 and Ruti et al., 2016; Cavicchia et al., 2018; Dell'Aquila et al., 2018 for more details about these model simulations) will be considered to provide an estimate of the projected changes of the Euro–Mediterranean climate in terms of changes in mean season values of near–surface temperature and precipitation.

Figure 5 shows the difference between seasonal averages for the period 2012-2050 with respect to the present climate (1971–2000) for the RCP4.5 emission scenario (IPCC, 2013). For near–surface temperature, all of the simulations agree for the period in exam on a relevant increase of mean temperature that can reach in summer the +2 degrees over the Mediterranean coasts. A relevant meridional gradient can be highlighted between the central and southern Europe in summer. During winter, the warming seems to be more evident in the Eastern Europe.
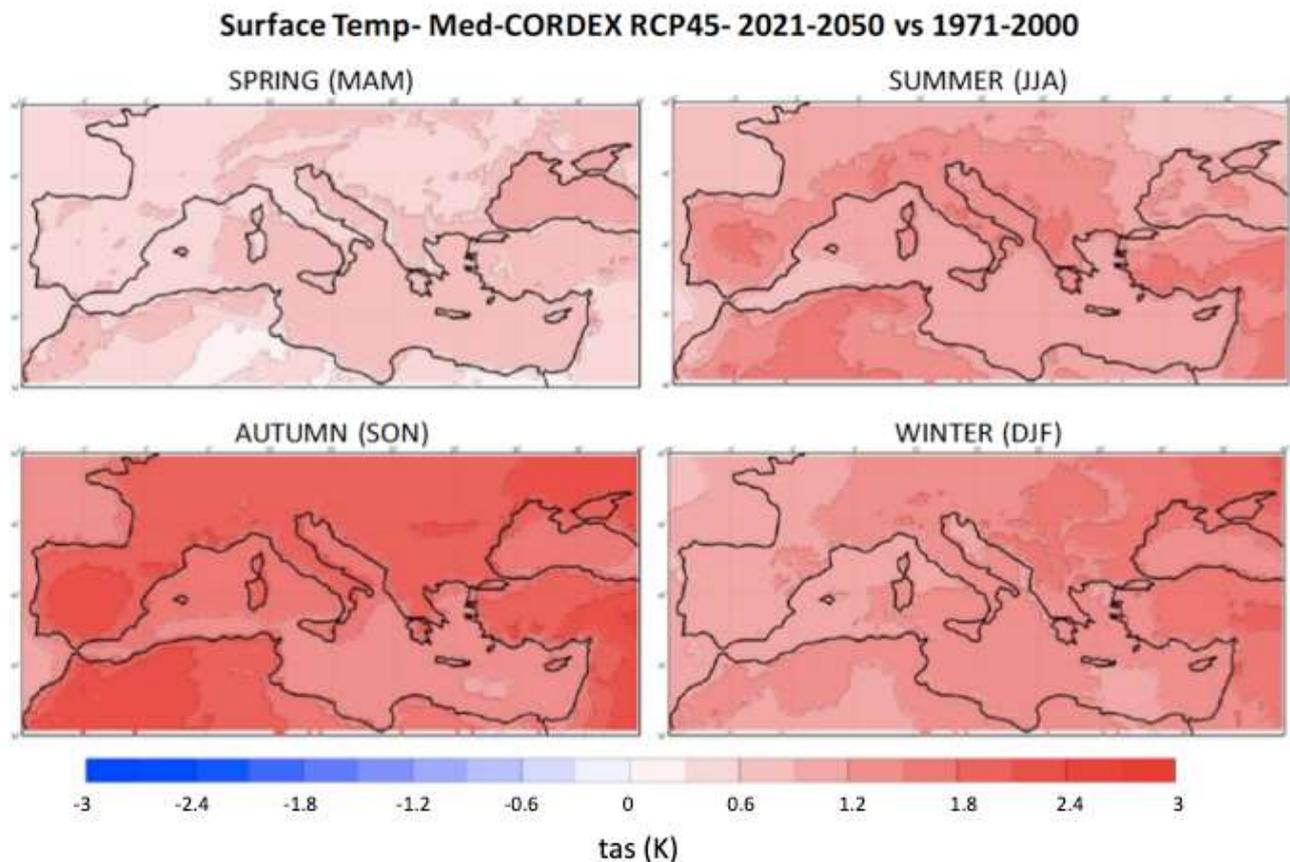

Figure 5. *Climate projections for the Euro-Mediterranean region from MED-CORDEX RCP45 simulations (see Table 2). Anomalies averaged over the period 2021-2050 with respect to the reference period 1971–2000 for Surface Temperature.*

For precipitation (Figure 6), the RCM simulations exhibit a weaker agreement (not shown). However, a relevant meridional gradient in the projected changes in the mean precipitation is present for all the seasons, with reduced mean precipitations for the Mediterranean region and a corresponding increase for northern-central Europe. In particular, over southern-central Italy the projections foresee a strong reduction of rainfall, while in the north the simulations do not agree on the sing of change, beside in spring when a strong decrease of mean precipitation is found even in the southern side of Alps.

13.2.2 Projected changes of extreme events in the Euro–Mediterranean area

Changes in the frequency and intensity of extreme events can seriously affect human society in a variety of ways. Therefore, it is important to provide assessments of potential changes in the tails of the temperature and precipitation distribution in possible future climates, making use of the

twenty-first century projections carried out with state-of–the–art coupled general circulation models (CGCMs) within the fifth Coupled Model Intercomparison Project (CMIP5, Meehl and Bony, 2011; Taylor et al., 2012). These simulations, in fact, provide the opportunity to investigate possible future changes in intense precipitation or heat wave occurrence following Representative Concentration Pathways (RCPs) considered as illustrative of potential future radiative forcing scenarios.
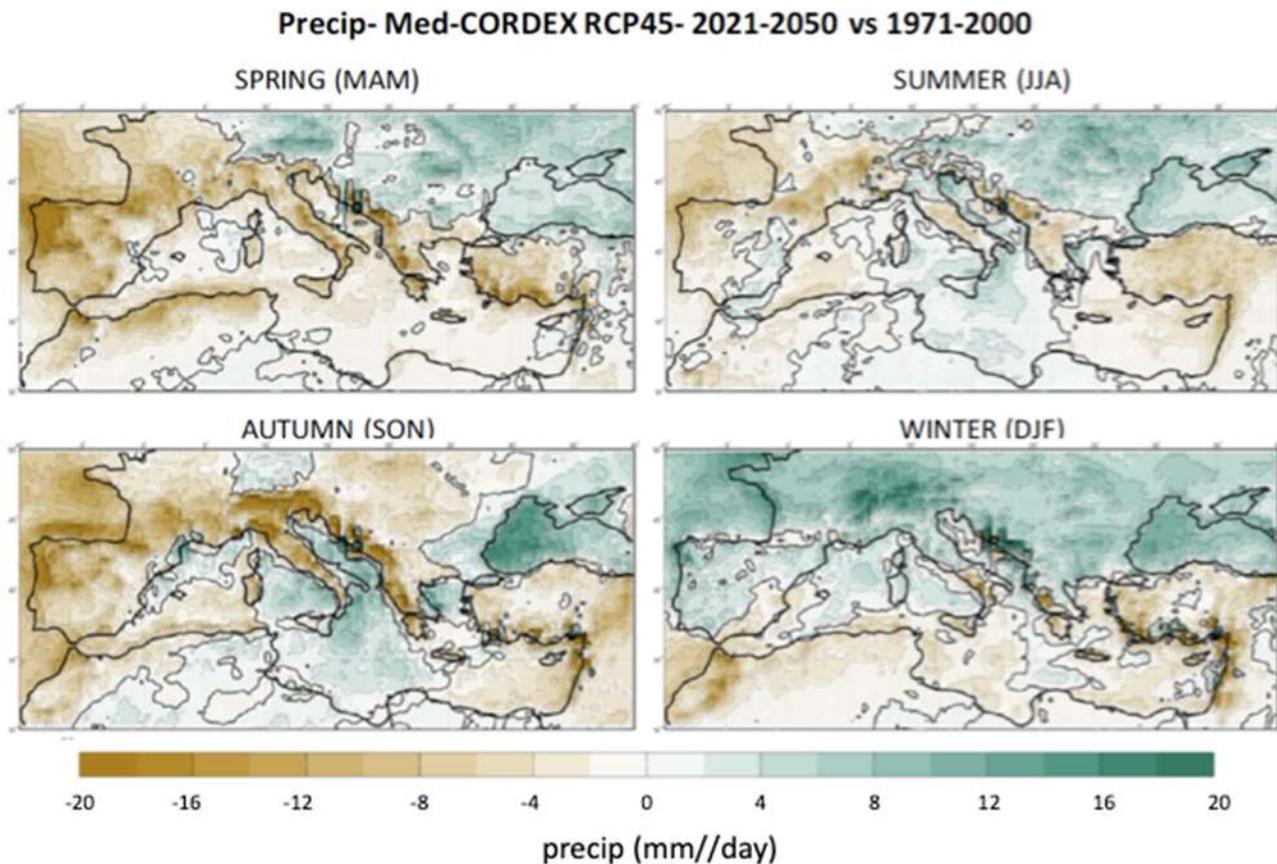
Precip- Med-CORDEX RCP45- 2021-2050 vs 1971-2000

Figure 6. As in Figure 5 but for projected precipitation (a) and precipitation (b) are here reported. For precipitation, in the dotted regions at least 2/3 simulations agree on the sign of foreseen changes (for temperature all the simulations agree on an overall warming).

Within the NextData project, an analysis aimed at exploring possible changes in the shape of the right tail of the precipitation distribution (intense and extreme precipitation events) under warmer conditions over the Euro-Mediterranean region has been conducted (Scoccimarro et al., 2016). The analysis has been performed using daily precipitation data from a sub–set of the CMIP5 multi-model ensemble, consisting of simulations of the twenty and twenty-first century climate performed with 20 coupled ocean–atmosphere climate models (see Scoccimarro et al., 2016, Table 1). Since the aim of this work was to assess potential changes in precipitation extremes that might have a societal impact, the analysis has mainly focused on precipitation overland.

The horizontal resolution of the atmospheric component of the considered models ranges from about 0.75° to about 3.5°, with a median of 1.7°. Two periods are analysed: 1966–2005 (hereafter PRESENT), corresponding to the last part of the 'historical' CMIP5 simulation; 2061–2100 (hereafter FUTURE). The future climate simulations here considered have been conducted under the high-end RCP8.5 scenario (Riahi et al., 2011). In order to provide a sufficiently representative sample for

intense events, a 40–year long record for each model and scenario has been considered. The 'historical' simulation has been performed forcing CMIP5 models with observed concentrations of greenhouse gasses, aerosols, ozone and solar irradiance, starting from an arbitrary point of a quasi-equilibrium control run. The RCP8.5 scenario follows a rising radiative forcing pathway leading to 8.5 W/m2 in 2100 corresponding to a carbon dioxide (CO_2) atmospheric concentration more than doubled if compared to the present period.

The capability of the CMIP5 models to simulate the statistics of heavy precipitation events in present climate conditions has been assessed using daily data from the Global Precipitation Climatology Project (GPCP, Bolvin et al., 2009) and from the E-OBS data set (Haylock et al., 2008) over the period 1997–2005. The horizontal resolution of the two observational data sets varies from 1° (GPCP) to 0.25° (E–OBS).

To assess how good CMIP5 models are in representing the right tail of the precipitation distribution when compared to observations, the analysis has been conducted on the simulated and observed 90th (90p) and 99th (99p) percentiles (Scoccimarro et al., 2013) obtained by aggregating daily precipitation values, belonging to the investigated period, over each single grid point. Changes in the intensity of heavy precipitation events, defined as daily events with a precipitation amount greater than 90p, are estimated through a simple metric based on the difference between 99p and 90p, where the former is representative of extreme precipitation and the latter is the threshold used to identify a heavy precipitation event. This metric is defined, separately for PRESENT and FUTURE climates, to quantify the width of the right tail of the precipitation distribution. Percentiles are computed for each observational data set and model on the corresponding original spatial grid. Individual results are then interpolated onto the GPCP regular grid to allow the graphical comparison and the multi-model averaging. Hereafter, the differences between FUTURE (2061–2100) and PRESENT (1966–2005) periods will be referred to as future changes.

The 99p–90p pattern over the Euro-Mediterranean region diagnosed for the 1997–2005 period from observations (E–OBS and GPCP) and CMIP5 models (ensemble mean) is shown in Figure 7. Noteworthy, in winter, the inconsistencies between the two observational data sets are particularly pronounced. It is also important to consider the very poor data coverage affecting the southern parts of the E–OBS domain (see Figure 1 in Haylock et al., 2008), which reduces the reliability of E–OBS data as verification set for the 99p–90p diagnostic over the southern Europe (see, as an example, the discrepancies between GPCP and E–OBS over Portugal). Moreover, the left and central part of the probability density function of the modelled precipitation appears to be underestimated, with an excessive number of simulated events associated to moderate and low precipitation rates (see Scoccimarro et al., 2016, Figures 3, 4, 5).

Overall, Scoccimarro et al. (2016) show a broad consistency between the observed and modelled 99p–90p patterns.

Projected changes in the climatological precipitation (shown in Figure 8, left panels) at the end of the twenty-first century are qualitatively consistent with similar analyses obtained using Coupled Model Intercomparison Project Phase 3 (CMIP3) models (Giorgi and Bi, 2009; Gualdi et al., 2013). In winter, a general increase (decrease) in precipitation overland is found over the Euro-Mediterranean domain, north (south) of 45N. In summer, a similar bipolar pattern is found but with

a zero-line around 55N–60N. Future changes in 90p (Figure 8, central panels) display a pattern highly spatially correlated with the corresponding pattern for the average precipitation.

The 99p–90p projected changes (Figure 8, right panels), show a different pattern compared to the climatological precipitation and 90th percentile spatial distributions. In the FUTURE period, in fact, the 99p–90p metric increases in almost the entire domain, including regions where average precipitation and 90p values show a decrease (red patterns in Figure 8).
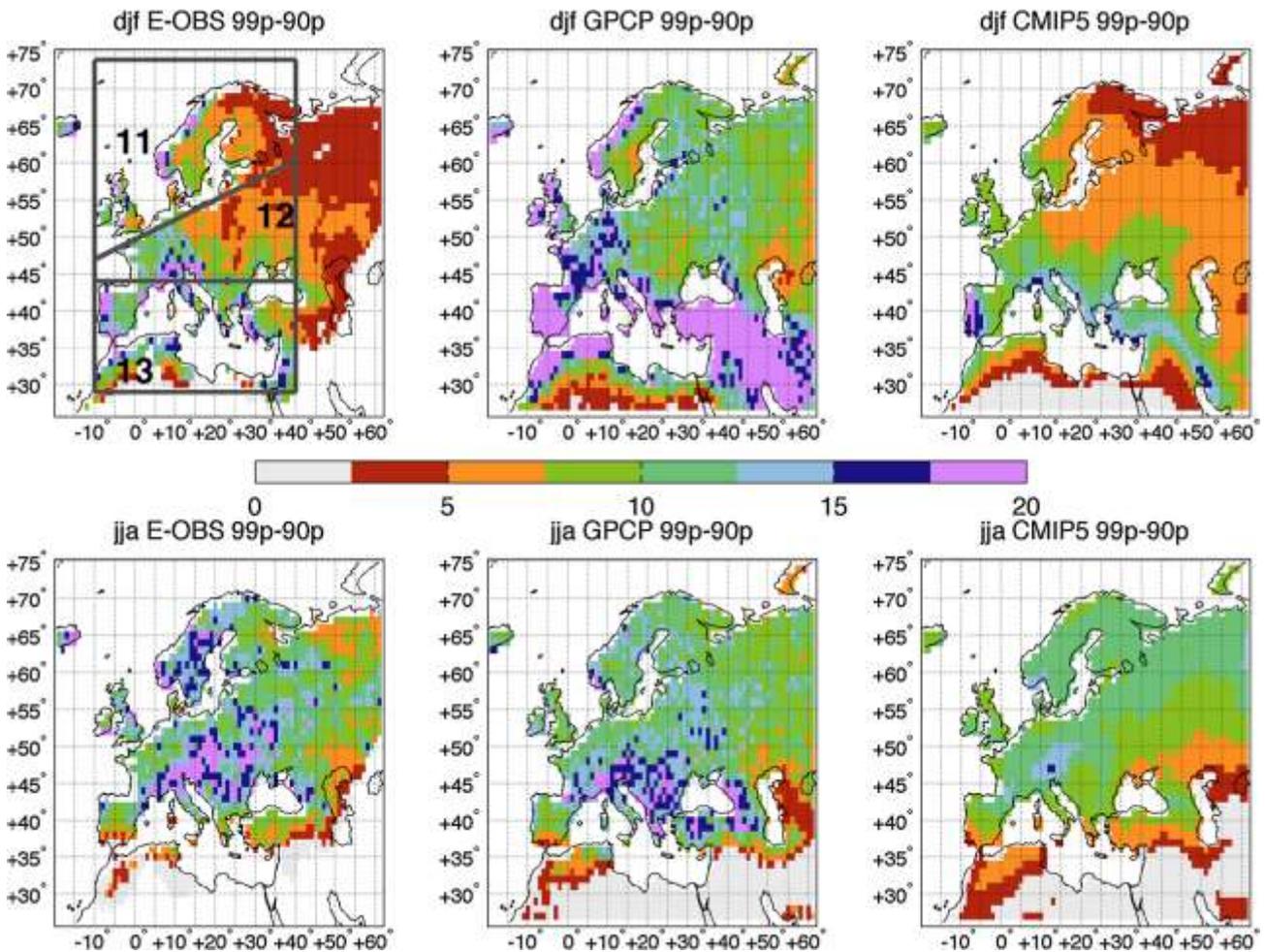

Figure 7. *Measure of the right tail of the precipitation events distribution, represented as the difference between 99th and 90th percentiles (99p–90p) during the period 1997–2005. Left column panels E-OBS observations, central column panels GPCP observations, right column panels CMIP5 (average over the 20 models), upper panels refer to boreal winter and lower panels refer to boreal summer. Units are (mm/day). In the top-left panel, regions 11/12/13 used for the regional diagnostics. For more details see Scoccimarro et al. (2016).*

This is the case of central and eastern Europe in summer, where the width of the right tail of the distribution increases, even if nearly, the entire precipitation distribution becomes dryer (i.e., decreases in total, 90p, and 99p precipitation). This positive tendency is then more pronounced for the rightmost part of the precipitation distribution and less pronounced for the remaining part of the precipitation distribution.

Scoccimarro et al. (2016) also assessed the long–term tendencies for the 99p–90p metric, grouping precipitation data over three European regions (northern/central/southern) selected following the IPCC special report on extreme events (IPCC 2012), corresponding to their regions 11/12/13 (their Figure SPM.4b and Figure 7, top-left panel). Both in DJF and JJA, northern and central Europe, show

a positive increment of the 99p–90p index (see Figures 3, 4 and 5 in Scoccimarro et al., 2016). On the other hand, changes over the southern part of the domain are more consistent with those found for the mean precipitation (red patterns in Figure 8).
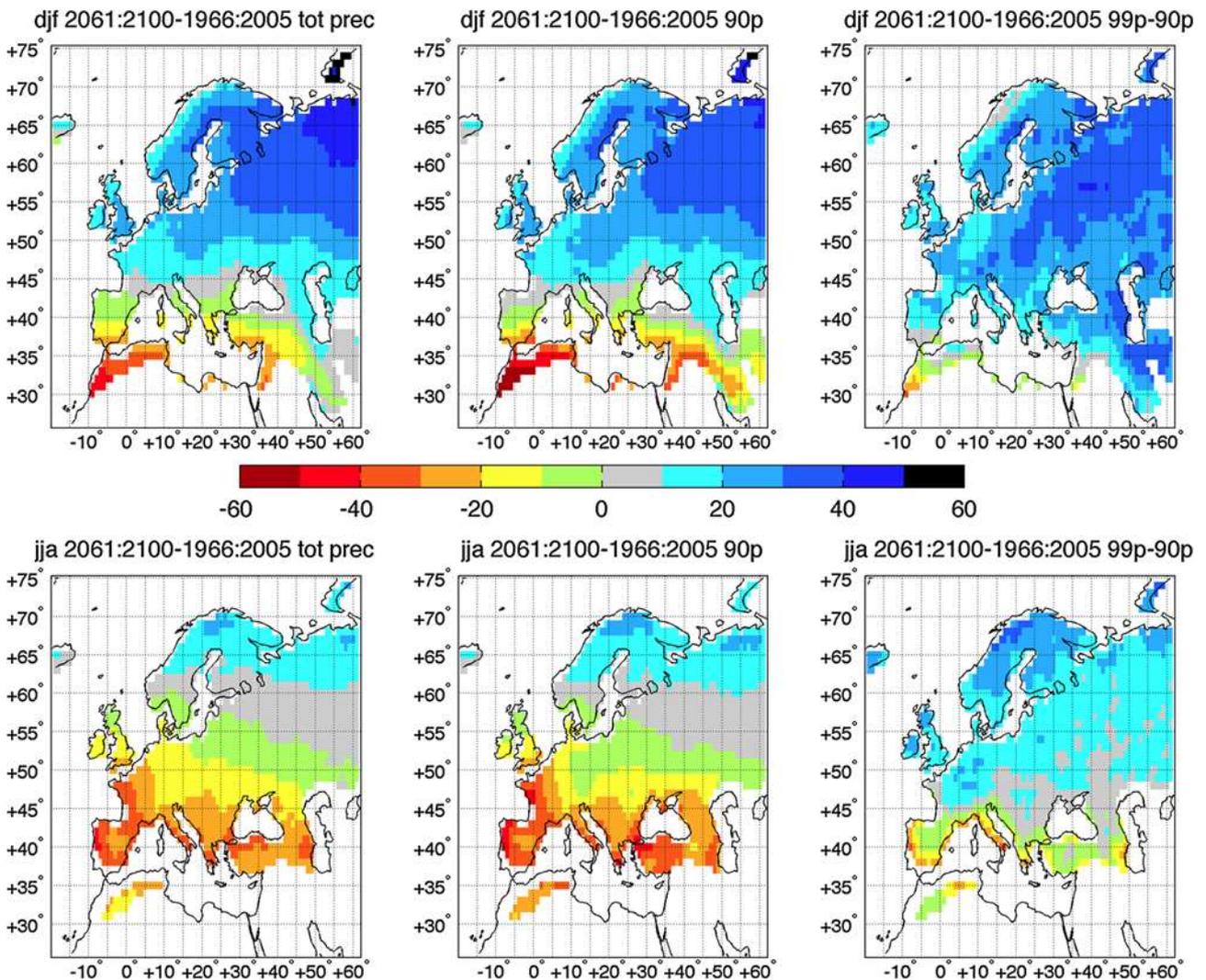

Figure 8. Future changes (2061–2100 to 1966–2005) in average precipitation (left panels), 90th percentile of precipitation (90p, central panels) and width of the right tail of the precipitation events distribution (99p–90p, right panels) following the RCP8.5 CMIP5 scenario, as averaged over the 20 CMIP5 models. Upper panels refer to boreal winter and lower panels refer to boreal summer. Units are (%). White patterns overland indicate regions with seasonal precipitation lower than 0.5 mm/day. For more details see Scoccimarro et al. (2016).

Noteworthy, the spread between 99p and 90p model projections is low: the projected results are very similar (not shown) even considering random sub–sampling of 10 models within the 20 models available.

In summary, within the NextData project, the difference between 99th and 90th percentile of the daily precipitation resulting from a set of 20 CMIP5 projections has been analysed, with the aim of quantifying potential changes in the width of the right tail of precipitation distribution. This diagnostic helps in quantifying, at the local scale, how much extreme values (>99p) deviate from the most frequently occurring conditions in a given climate, providing valuable information for

managing activities, as for example infrastructure design, where the occurrence of extraordinarily intense meteo–climatic events needs to be accounted for.

The intensity of heavy precipitation events seems to increase more than mean precipitation under a warmer climate, over a substantial portion of the Euro–Mediterranean domain, confirming previous findings (e.g., Chou et al., 2009). These changes are consistent with a greater moisture holding capacity of the warmer air contributing to greater moisture convergence (Tebaldi et al., 2006) and with the Clausius–Clapeyron law, relevant for heavy precipitation events (Giorgi et al., 2011), which are able to significantly reduce the atmospheric moisture column (Allan and Soden, 2008).

Therefore, CMIP5 model projections for the end of the twenty-first century under a radiative forcing scenario with no mitigation efforts indicate that Euro-Mediterranean region might be characterized by intensified heavy precipitation events over the majority of land, especially during winter. This implies increasing risks of natural and human systems that are sensitive to wet extremes. On the other hand, during summer, both heavy and extreme precipitation events are projected to be reduced over southern Europe (see also Rajczak et al., 2013 and references therein).

In this section, for the sake of brevity, we focused on Euro–Mediterranean precipitation extremes. On the other hand, within the NextData project, similar studies have been conducted to explore temperature extremes (heat waves), as, for example, in Zampieri et al. (2016).

13.2.3 Climate change projections over the Italian Peninsula

The Italian Peninsula is characterized by a very complex topography, ranging from high mountain chains to a very diverse coastline, being almost totally surrounded by the Mediterranean Sea. This geomorphological configuration makes the representation of the different local climate patterns challenging for numerical models. Furthermore, spatial resolution of state–of–the–art GCMs is generally too coarse to properly represent the complexity of the geomorphology of the region. Consequently, simulations performed with GCMs are in most cases unable to reproduce many processes that drive local climate variability. For this reason, climate change scenarios for the Italian Peninsula are generally performed and produced using high–resolution limited area models, such as those employed in the already mentioned CORDEX (Euro–CORDEX and Med–CORDEX) programmes or in European projects such as PRUDENCE (http://prudence.dmi.dk/, and ENSEMBLES (Van Der Linden, 2009).

Coppola and Giorgi (2010), for example, provided an exhaustive assessment of climate change projections over Italy, according to a number of global and regional high–resolution models, and considering different emission scenarios (see Coppola and Giorgi, 2010, for more details). Overall, the models indicate a warming, up to several degrees in the most intensive emission scenarios, in all seasons at the end of the 21st century. Precipitation is projected to decrease over the entire domain in summer and, to a lesser extent, in spring and fall, whereas it increases in winter over northern Italy.

More recently, Montesarchio et al. (2014) performed several simulations with the RCM COSMO–CLM over the Italian Peninsula, which have been then analyzed in terms of mean climate change and trends (Bucchignani et al., 2015). Specifically, three simulations driven by ERA-Interim

Reanalysis were conducted at a spatial resolution respectively of 0.22° (about 25 km), 0.125° (about 14 km) and 0.0715° (about 8 km) over the period 1979–2011. Besides, two simulations at a spatial resolution of 0.0715° driven by the GCM CMCC–CM (Scoccimarro et al., 2011) were performed over the period 1971–2100, using the IPCC RCP4.5 and RCP8.5 emission scenarios.

Bucchignani et al. (2015) show that these high-resolution simulations allow a satisfactory representation of the Italian climate, biases being lower than (or comparable to) values that affect state–of–the–art regional climate simulations (i.e. Euro–CORDEX data at 0.11°) with a high detail level, not obtainable with coarser resolutions. Bucchignani et al. (2015) analysed also climate projections as obtained using the RCP4.5 and RCP8.5 emission scenarios.

Figure 9 shows the T2m seasonal change projections for the period 2071–2100 with respect to 1971–2000 for the RCP8.5 scenario.
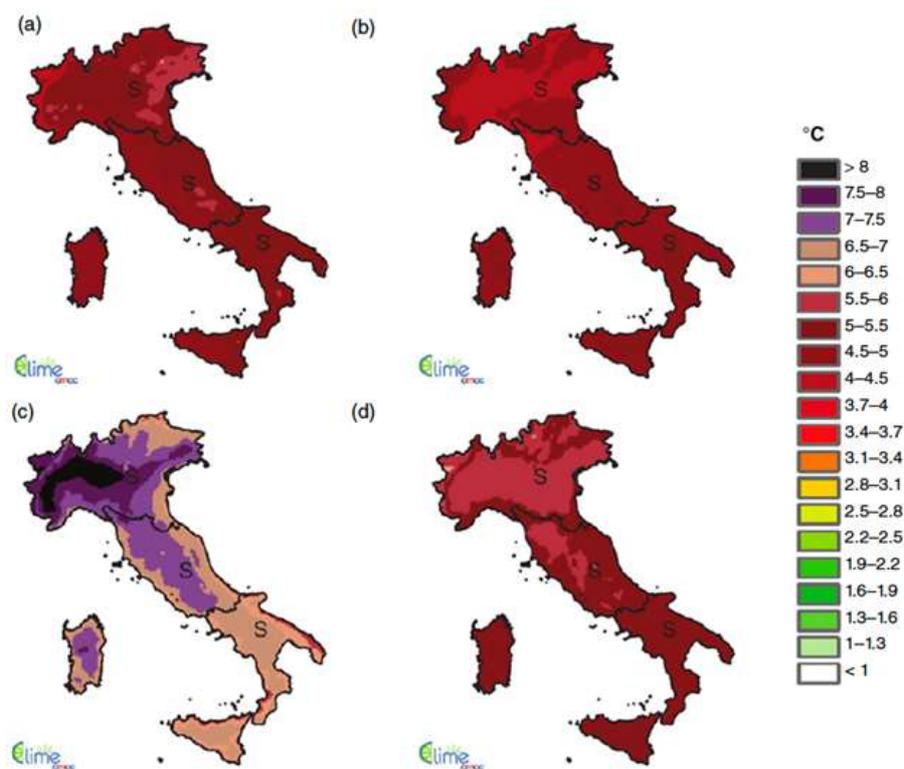

Figure 9. *Temperature climate projections, RCP8.5: seasonal differences (∘C), between the average value over 2071–2100 and 1971–2000 for (a) DJF, (b) MAM, (c) JJA and (d) SON (S, significant; NS, not significant). From Bucchignani et al. (2015).*

A general temperature increase of about 4 °C is projected in all seasons, over the whole of Italy; peaks as large as 8 °C are projected over the western part of the Po Valley in summer and, in general, during this season, the most of the Peninsula appears to be more than 6 °C hotter than the reference climate.

When the less intense radiative forcing scenario RCP4.5 is considered, a weaker warming is projected over the Italian Peninsula (not shown), characterized by a temperature increase of about 3 °C is projected in all seasons, over the whole of Italy; peaks of 4 °C are projected over the Po Valley in winter and over the whole north-west area in summer.

These temperature–projected changes are statistically significant over the whole of Italy, for both scenarios, according to a Mann–Kendall nonparametric test with a confidence level of 95%.

Figure 10 shows the precipitation change projection for the period 2071–2100 with respect to 1971–2000 for the RCP8.5 scenario: a significant increase in precipitation is projected in winter over northern Italy and over the central–western part of the Peninsula. Central–eastern and northern Italy, on the other hand, appear to be affected by a strong significant precipitation reduction in summer, particularly evident in the Alpine area. In the projections, the whole of the Italian Peninsula appears to be affected by a significant reduction in spring, especially in high mountain areas, whereas in fall only the Apennines show a precipitation reduction.
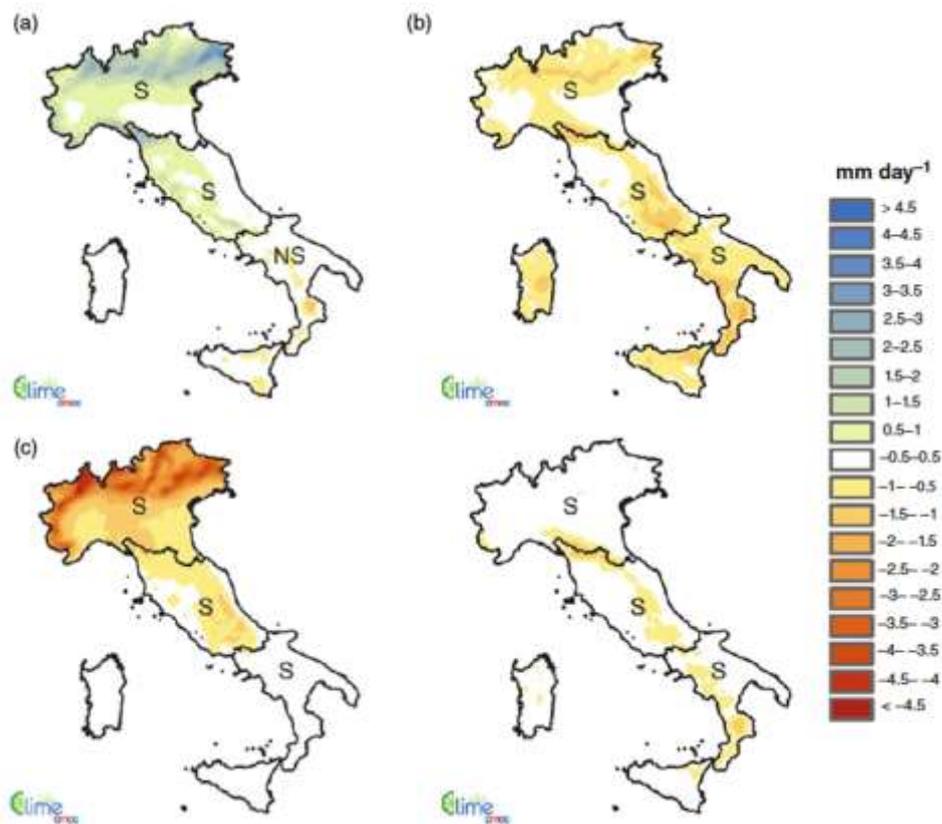

Figure 10. Precipitation climate projections, RCP8.5: seasonal differences (mm day−1), between the average value over 2071–2100 and 1971–2000 for (a) DJF, (b) MAM, (c) JJA and (d) SON (S, significant; NS, not significant). From Bucchignani et al. (2015).

In the RCP4.5 scenario (not shown) a moderate, non-significant, increase in precipitation is projected in winter over the eastern Alpine area, while a significant decrease is produced in summer over northern Italy. Significant reductions are projected also in MAM, in central and southern Italy. Annual mean temperature and precipitation time series (5-year running mean) and trend lines for northern, central and southern Italy are shown in Figure 11 and Figure 12, respectively. These figures show a a marked general warming projected over the whole Italian Peninsula in the course of the 21st century, producing a warming in all of the considered subareas that at the end of the century is of about 3.2 °C in the RCP4.5 scenario, and about 6.3 °C in the RCP8.5 scenario.

Temperature projected changes are statistically significant and consistent with others results obtained with both global and regional models (e.g. Coppola and Giorgi, 2010), for different emission scenarios. The warming is accompanied by a general reduction of mean precipitation (Figure 12), more pronounced in the RCP8.5 scenario. The overall reduction of precipitation, along with the increase in DJF over northern Italy (see Figure 10), is in agreement with projections

described by Giorgi and Lionello (2008), and is due to circulation change patterns (increasing anticyclonic circulation) that will affect the whole Mediterranean region (e.g., Gualdi et al., 2013). A good qualitative agreement is registered also with projections described by Coppola and Giorgi (2010), where a substantial drying is expected in summer, while in winter the signal presents a dipolar pattern with an increase in the northern region and a decrease in the south.
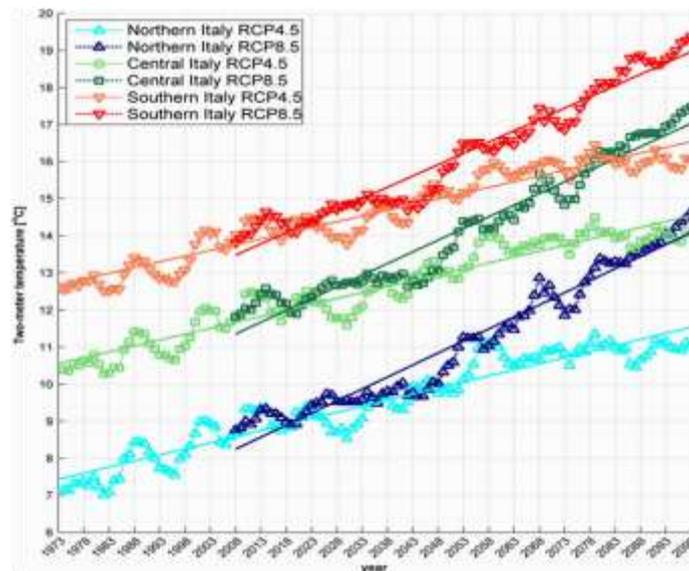

Figure 11. *Time series of T2m and trend lines (C°) over Northern, Central and Southern Italy (5-year running mean) for the RCP4.5 and RCP8.5 scenarios (from Bucchignani et al., 2015).*

Overall, precipitation data extracted by EURO-CORDEX RCMs project no significant variations over Italy for RCP4.5 (+0.1, 0 and −0.1mmday−1 respectively over North, Centre and South) and larger reductions for RCP8.5 in Centre and South (0, −0.2 and −0.3 mmday−1) in qualitative agreement with the results of the present work.
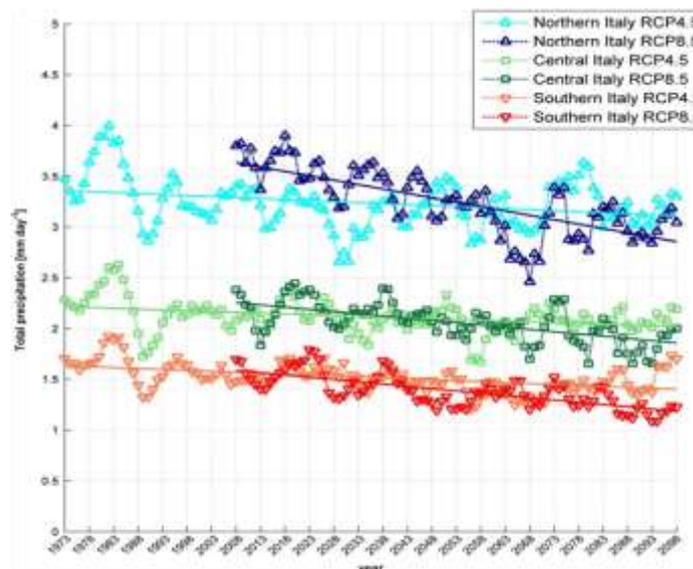

Figure 12. *Time series of precipitation and trend lines (mm day−1) over Northern, Central and Southern Italy (5-year running mean) for the RCP4.5 and RCP8.5 scenarios (from Bucchignani et al. 2015).*

Finally, when possible changes of extreme precipitation events over Italy projected by the Med–CORDEX models are considered, results appear to be less robust. As an example, in Figure 13 we report the projected changes in Med–CORDEX RCP4.5 simulations in the occurrence of intense precipitation events over a box covering the Italian peninsula for all seasons. Intense events have been here defined as those whose anomaly values exceed the 95p threshold (95th percentile), as obtained from the reference seasonal cycle of present climate in each simulation.
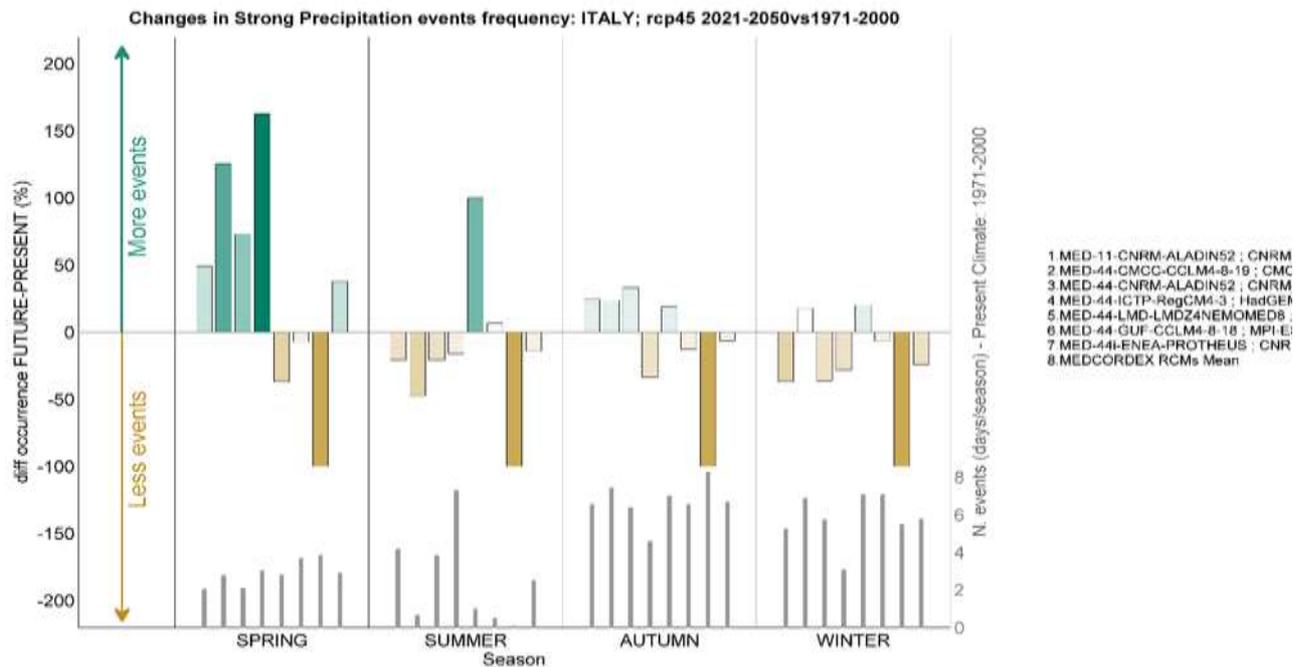

Figure 13. *Histograms of MED_CORDEX RCP45 simulations for projected changes (2021–2050 against 1971–2000) in the occurrence of intense precipitation events over Italy. Intense events have been here defined as those whose anomaly values exceed the threshold (95th percentile) from the reference seasonal cycle of present climate as described in each simulation. The colour bars indicate the changes in the occurrence (%) of the above defined intense events in each RCM simulations (here reported on the right with the corresponding global drivers) considered for different seasons. The thin grey lines are for the number of events in the reference 1971-2000 period.*

As the results in Figure 13 show, in all of the seasons, the Med–CORDEX RCMs simulations do not fully agree in the projected changes of occurrence of intense perturbations. However, most part of the simulations foresee less intense rainy events during summer. On the other hand, in most of the considered simulations, an increase of strong precipitation events during spring (and to a lesser extent autumn) can be found.

13.3 Expected climate change in Italian mountains

In the following we will provide an analysis of the capability of numerical climate simulations to reproduce the main features of the observed climate in areas characterized by complex orography, such as the Italian mountains and in particular the Alpine region. The improvements in the simulated climate related to the use of very–high resolution models will be discussed and an assessment of the climate change signal in the Alpine area produced by these models will be provided.

13.3.1 Evaluating high–resolution climate models in Italian mountain regions

Zollo et al. (2015) have explored the ability of a climate model to reproduce the main climatological features of a sub–set of the ETCCDI (Expert Team on Climate Change Detection and Indices) indices for precipitation (Karl et al., 1999), in a region with complex orography. In particular, the study has assessed the performance of an atmospheric RCM (COSMO-CLM, Rockel et al., 2008), implemented with two horizontal resolutions (0.125° and 0.0715°), extensively used to produce climate simulations for the Alpine region in the framework of the NextData project. The COSMO model, in these experiments, has been integrated both with "perfect boundary conditions" from ERA–Interim reanalysis (Dee et al., 2011) and in suboptimal conditions, i.e. using boundary conditions obtained from the global coupled model named CMCC–CM (Scoccimarro et al., 2011). The comparison between the two configurations allows to identify the systematic errors due to the RCM model and the biases introduced by potentially erroneous large–scale forcing.

The considered indices are:

- SDI: Simple precipitation intensity index
- CDD: Maximum length of dry spell, i.e. maximum number of consecutive days with RR < 1mm;
- CWD: Maximum length of wet spell, i.e. maximum number of consecutive days with RR ≥ 1mm:
- Rx1day: Monthly maximum 1-day precipitation;
- Rx5day: Monthly maximum consecutive 5-day precipitation;
- R10: Annual count of days when daily Precipitation ≥ 10mm;
- R20: Annual count of days when daily Precipitation ≥ 20mm;
- 99p: Annual total PRCP when RR > 99p;
- 90p: Annual total PRCP when RR > 90p.

Figure 14 shows the model bias when compared to the EURO4M observational dataset (Isotta et al., 2014), a gridded, high–resolution daily precipitation dataset in the Alps obtained from pan-Alpine rain-gauge data. In most of the cases, results indicate an overall tendency of the model to underestimate the value of the indices, with the exception of the number of consecutive dry days (CDD).

When the spatial pattern of the bias is considered, Figure 15, then it emerges that extreme indices tend to be overestimated over the Alpine mountainous chain, and underestimated over surrounding areas. The model has some difficulties in reproducing correctly the observed variability for consecutive dry and wet days in the Alpine area. Indeed, it tends to accentuate the difference between the number of rainy days over the Alps (overestimated) and over the surrounding flat areas (underestimated).

In terms of improvement related to resolution, it is difficult to draw a general conclusion: precipitation indices that benefit more from the resolution increase for all regions are CDD, Rx1day and Rx5day, which are very interesting indicators for impact studies. In terms of temperature, the indices based on minimum temperature are generally improved, while indices based on maximum temperature behave differently, depending on the region considered. It is important to note a strong dependent on the region, especially in topographically complex areas. On average, for most

indices and regions, the increase in resolution leads to a better representation of climate patterns, indicating that a higher resolution helps to better simulate smaller scale and higher variability events (Vautard et al., 2013). However, in mountainous areas it is more difficult to detect improvements due to parameterization problems, since the 0.0715° resolution is still too coarse to allow convection to be simulated without parameterizations (Wulfmeyer et al., 2011).
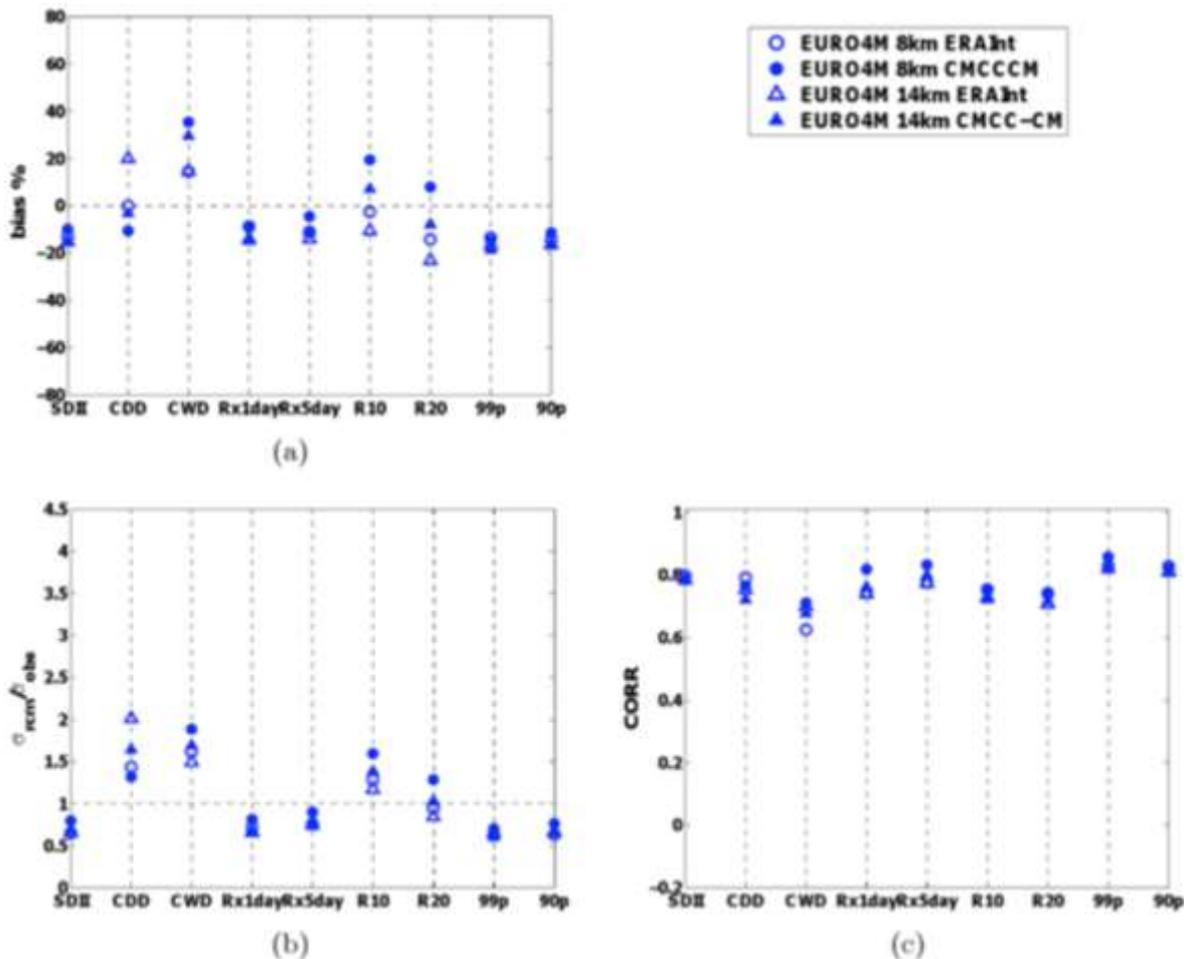

Figure 14. *Overall systematic error of the COSMO-CLM simulations (Montesarchio et al., 2014) against the EURO4M-APGD data set for the considered precipitation indices over the Alpine region. The error measures are (a) percentage bias, (b) ratio between the standard deviation of RCM data and observations and (c) spatial correlation.*

Although biases are still not negligible, COSMO-CLM allows a satisfactory representation of extreme indices of temperature (not shown) and precipitation over Italy. As regards the improvement introduced by higher resolution, this analysis is not entirely conclusive. Indeed, despite some overall ameliorations due to a model finer resolution, the increase in resolution does not generally involve a clear benefit for a correct representation of all the extreme indices considered. It is worth noting that the difference between the two resolutions here considered (14 km and 8 km) is rather small and this could be the cause of the quite heterogeneous picture, without a significant improvement for 8 km simulations. A more in depth analysis of the possible benefits associated with a better model resolution is provided in the next Section.

12.3.2 Evaluating benefits of improved model resolution in simulating Italian mountain region climate

Evaluating the benefit of higher resolution models represents a relevant issue in different contexts, but it is even more so for mountain areas that represent a considerable field of challenge for RCMs, trying to reproduce mean climate and extremes, particularly for precipitation, in complex orographic contexts.
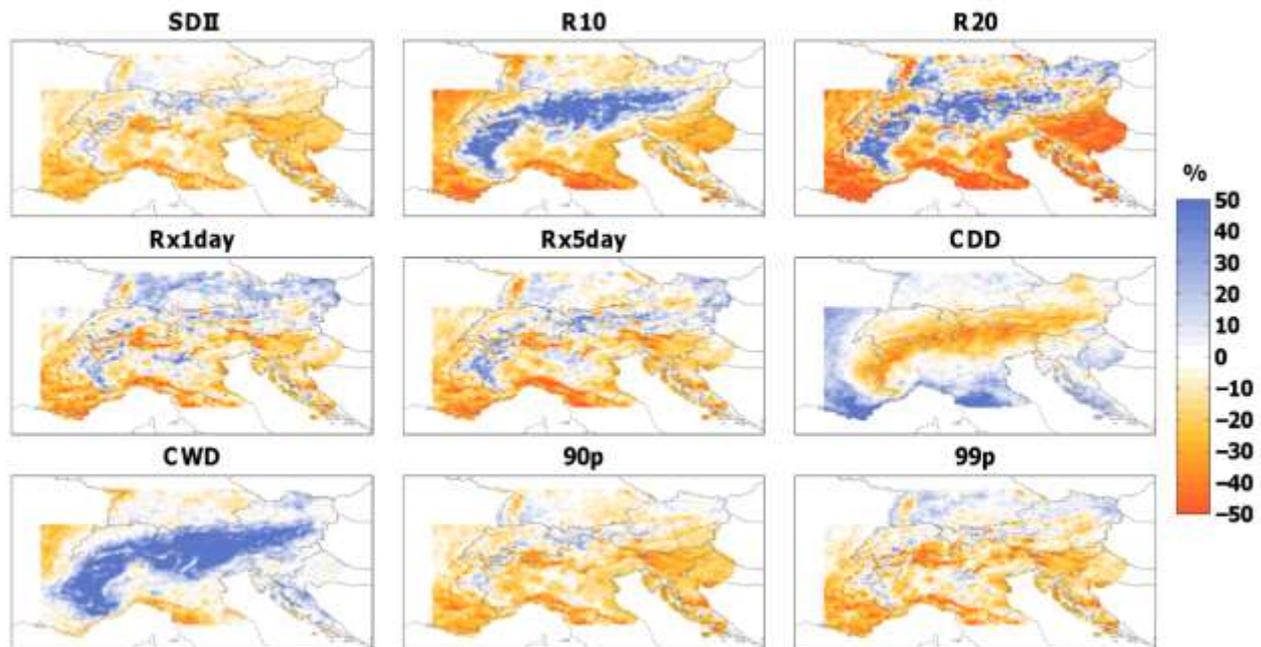

Figure 15. Spatial pattern of the bias of COSMO-CLM model against the EURO4M-APGD data set for the precipitation indices. The considered simulation is at 0.0715∘ of horizontal resolution and is forced by ERA-Interim reanalysis.

Over small mountain catchments, the precipitation events, especially those related to convective instability, could have a significant impact for their short–duration. Previous investigations have highlighted the inaccuracy of climate simulations – with deep convection parameterization and horizontal resolution in the order of 10 km – in reproducing such phenomena (e.g., Bucchighani et al., 2013; Jacob et al., 2015 and references there in). On the same topic, some studies have shown that very high resolution (VHR) simulations, about 1–3 km, could improve the models' capability to represent these phenomena, especially in complex orographic contexts, thanks also to the explicit treatment of the convective processes and a better representation of the orography (Ban et al., 2014; Prein et al., 2015).

Within the NextData project, activities have been carried out to investigate the performances of very–high resolution (VHR) simulations in terms of capability to represent daily and sub-daily precipitation dynamics. The main goal was to quantify objectively gains and losses related to the enhancement of spatial resolution, at different time scales, in simulating climate in regions with complex orography and especially in the Alpine Region.

In particular, the activity has been carried out considering climate simulations performed with different implementations of the RCM COSMO-CLM (Rockel et al., 2008) (Figure 16 and Table 2). The first configuration, named CCLM 8, is a climate simulation covering the Italian peninsula and part of the neighbouring areas, and characterized by a spatial resolution of 0.0715° (about 8 km) driven by boundary conditions taken from ERA-Interim.

The second model implementation, named CCLM 2.2, produced a finer climate simulation, with a spatial resolution of 0.02° (about 2.2 km) directly nested in CCLM 8 and covering a smaller area centred over the Alpine space. Both configurations are considered for the model evaluation at daily and sub-daily scales.
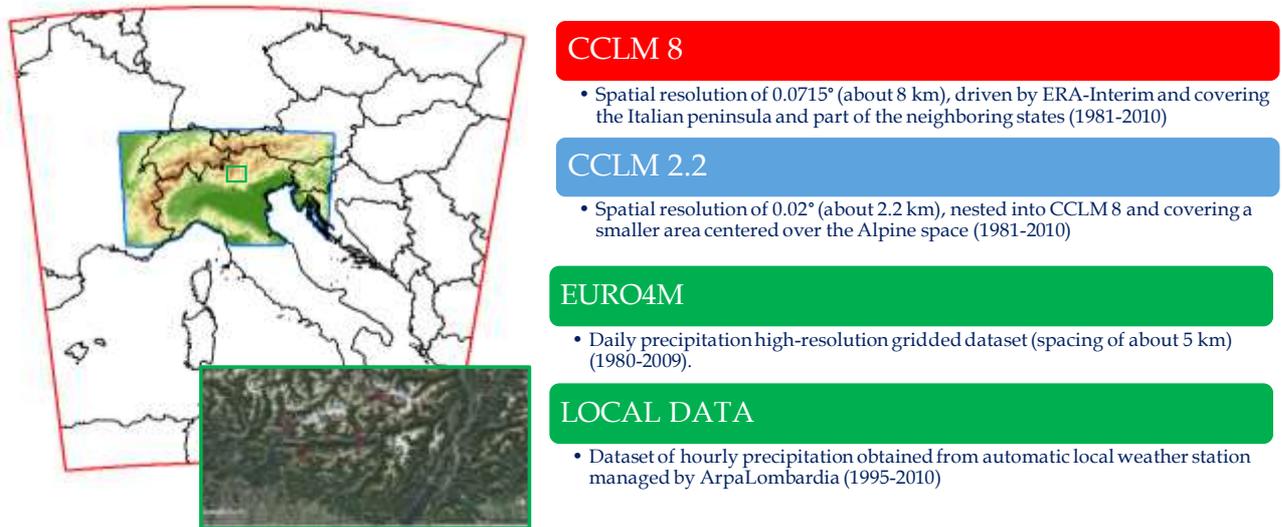

CCLM 8
- Spatial resolution of 0.0715° (about 8 km), driven by ERA-Interim and covering the Italian peninsula and part of the neighboring states (1981-2010)

CCLM 2.2
- Spatial resolution of 0.02° (about 2.2 km), nested into CCLM 8 and covering a smaller area centered over the Alpine space (1981-2010)

EURO4M
- Daily precipitation high-resolution gridded dataset (spacing of about 5 km) (1980-2009).

LOCAL DATA
- Dataset of hourly precipitation obtained from automatic local weather station managed by ArpaLombardia (1995-2010)

Figure 16. *Computational domain of CCLM 8 and CCLM 2.2; location of local station.*

The advantage of moving from a coarser resolution (8 km) to a finer one (2.2 km) consists principally in a better representation of real topography and the possibility of switching off the deep convection parameterization, improving the reproduction of the mesoscale circulation dynamics and the possible elevation dependencies of the near-surface climate change.

	CCLM 8	CCLM 2.2
Driving data	ERA-Interim Reanalysis	CCLM 8
Horizontal resolution	0.0715° (about 8 km)	0.02° (about 2 km)
Number of grid points	224 x 230	390 x 230
Time step	40 s	10 s
Convection scheme	Tiedke	Shallow convection based on Tiedke
Frequency of radiatio computation	1 hour	15 min
Maximal turbulent length scale	500 m	150 m
Critical value for normalized over saturation	4	1.6

Table 2. *Main differences between the implemented COSMO-CLM configurations.*

The accuracy of both climate simulations is evaluated at daily and sub-daily scales. For daily scale evaluation, the EURO4M (Isotta et al., 2014) dataset is considered (Figure 17, top panels). This is a high–resolution gridded dataset (spacing of about 5 km), covering the period 1971 e 2009, and obtained from high-resolution rain–gauge data, with a distance–angular weighting scheme that integrates climatological precipitation-topography relationships. For sub–daily scale evaluation, data provided by 11 local weather stations are considered (Figure 16, red dots, and Table 2). These

stations have been selected at different altitudes to account for the effects of orography and presented a time resolution of 1 hr. Data have been aggregated at time resolution of 6 hr that is the minimum common time resolution between CCLM 8 and CCLM 2.2.

Simulations have been analyzed over periods 1980-2008 for daily precipitation and 1995–2010 for sub–daily precipitation, each one obtained by a time intersection between model outputs and observed datasets; in the first case, the year 1979 has been neglected as it is considered as spin-up. All the daily datasets, remapped with bilinear interpolation over the EURO4m grids, have been processed considering a subset of the ETCCDI indicators mentioned above. In particular the following indices have been here considered:

- Rx1day (maximum 1–day precipitation),

- CWD (maximum length of wet spell)

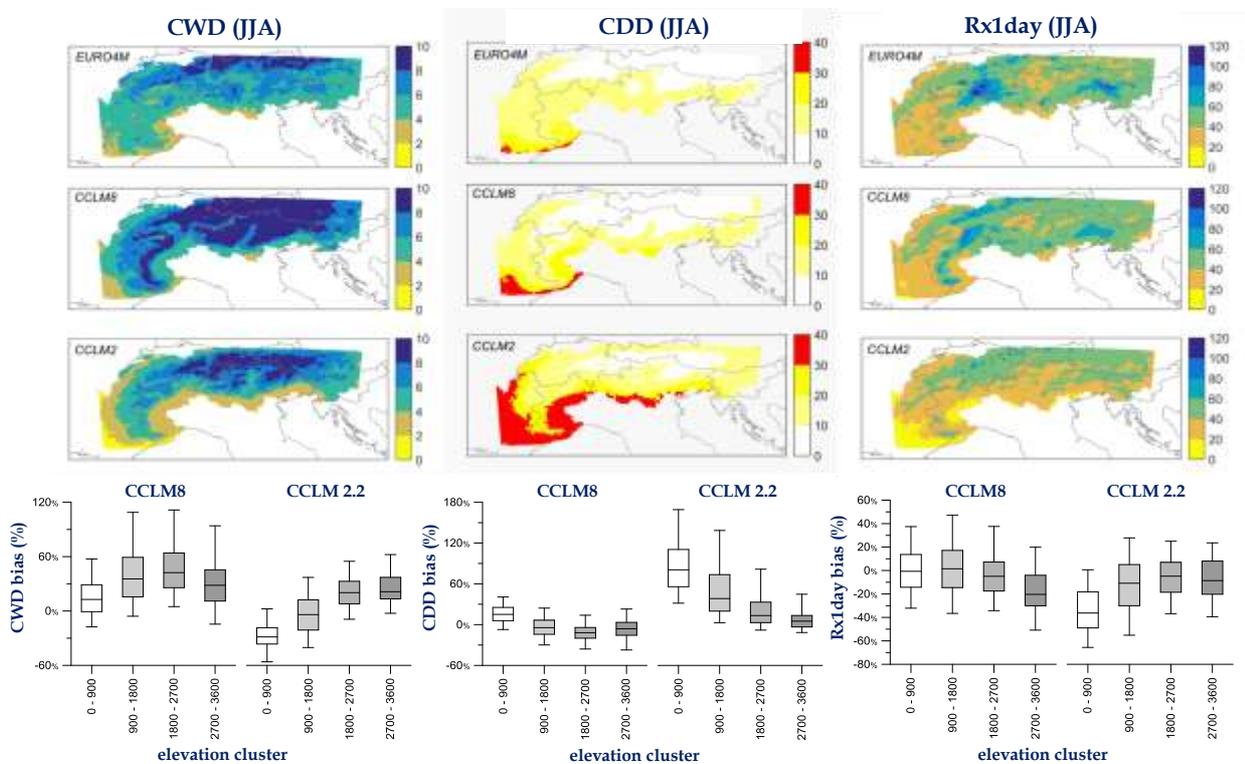- CDD (maximum length of dry spell).

Figure 17. *Upper panels: Comparison between EURO4M, CCLM8 and CCLM2.2 for CWD, CDD and Rx1day during June–July–August (JJA) for the period 1981–2009; Lower panels: The same comparison clustering results on the basis of grid–point (station) elevation (box-whisker plot diagram).*

Data have been elaborated as seasonal means for the seasons DJF (December–January–February) and JJA (June–July–August) assuming, as spatial boundaries, the delimitation suggested by the Alpine Convention for the Alpine region. In addition to this spatial study, all the indicators have also been clustered on the basis of altitude to investigate the effect of orography.

Regarding sub–daily analysis, the evaluation has been performed considering:

- sub–daily precipitation distribution fitting data through the Gamma function;
- extreme values for different duration of the precipitation events fitting data through GEV.

In this perspective, the position of local stations is considered to select a corresponding grid point from the CCLM 8.8 and CCLM 2.2 grids, using the nearest neighbour interpolation with a specific refinement for the CCLM 2.2 for which also an altitude constraint is introduced (Ban et al., 2014). Also in this case, data are elaborated for the seasons DJF and JJA.

ID	Station	Height (m a.s.l)	ID	Station	Height (m a.s.l)
108	Samolaco	206	832	Lanzada	2155
133	Bema	800	833	Gerola Alta	1845
567	Chiavenna	333	835	Valdisotto	2295
569	Sondrio	307	836	Aprica	1950
570	Tirano	439	848	Livigno	2655
571	Bormio	1225			

Table 3. *Local Weather Station Rx1day bias for CCLM 8 and CCLM 2.2; the minimum absolute value for each point isreported in red.*

To assess the performances of both climate projections and mainly to quantify objectively the added value in adopting high resolution RCMs, data obtained have been elaborated considering the distribution added value (DAV) as metric (Soares et al., 2017). Such a metric provides an objectively and normalized measure of the added value in terms of potential gain due to the higher resolution, comparing higher– and coarser–resolution simulation Probability Density Function (PDFs) mediated by the observational PDF. In this perspective, the DAV considers directly the Perkins skill score (Perkins et al., 2007) between high–resolution and low–resolution using observations as a reference.

Specifically, when DAV=0 indicates that no gain is found, DAV<0 indicates a loss associated to higher resolution and DAV>0 expresses a beneficial impact of a finer grid spacing on the PDF description. Some of the main results obtained from the analysis are shown in Figure 17, which shows the seasonal means of CWD, CDD and Rx1day indicators for JJA. For each indicator, the Figure reports also the percentage bias variation of both model configurations against observations; such a variation is represented in terms of box whisker plot clustered for different elevation ranges (Figure 17, bottom panels).

Comparing results of EURO4M, CCLM 8 and CCLM 2.2, CWD yields an added value from coarser to higher resolution (reduced bias), whereas Rx1day and especially CDD return an opposite behaviour. This is objectively assessed through the DAV: in terms CWD the gain in moving from CCLM 8 to CCLM 2.2 is +20%, whereas for CDD and Rx1day the loss associated to the higher resolution is -20% and -12%, respectively.

The clustering of the skill according to the elevation ranges (Figure 17, bottom panels) shows that for the CDD case there is a loss in accuracy for all elevations that, however, decreases with the altitude (from -38% for lower altitude to -14% for higher altitude). For CWD the DAV yields a gain for altitude ranging between 900-2700 m (up to +72%) and a loss for altitude lower than 900 m and higher than 2700 m (about -15%); finally, for Rx1day the loss of accuracy evaluated on the whole domain is due to events occurring at altitude lower than 900 m, whereas in the other case a gain is verifiable with the maximum gain for altitude higher than 2700 m (+13%).

These results show that, in mountain areas, some remarkable skill is already attained with the CCLM 8 simulation, even if some further improvement is obtained with the higher resolution model

version CCLM 2.2. Importantly, a possible burden of the evaluation provided by this analysis is due to the horizontal resolution of the observational dataset (5 km), which may not capture all the dynamics of the finer resolution simulations when the model is used with its higher resolution configuration (CCLM 2.2, 2.2 km).

Figure 18 shows some results from the sub-daily precipitation analysis. Specifically, it shows the elevation of local stations and corresponding grid points from CCLM 8 and CCLM 2.2, and the values of Rx1day for each local point and, as an instance, the Cumulative Distribution Function (CDF) of the Gamma Distribution for two local points (those characterized by the higher altitude).
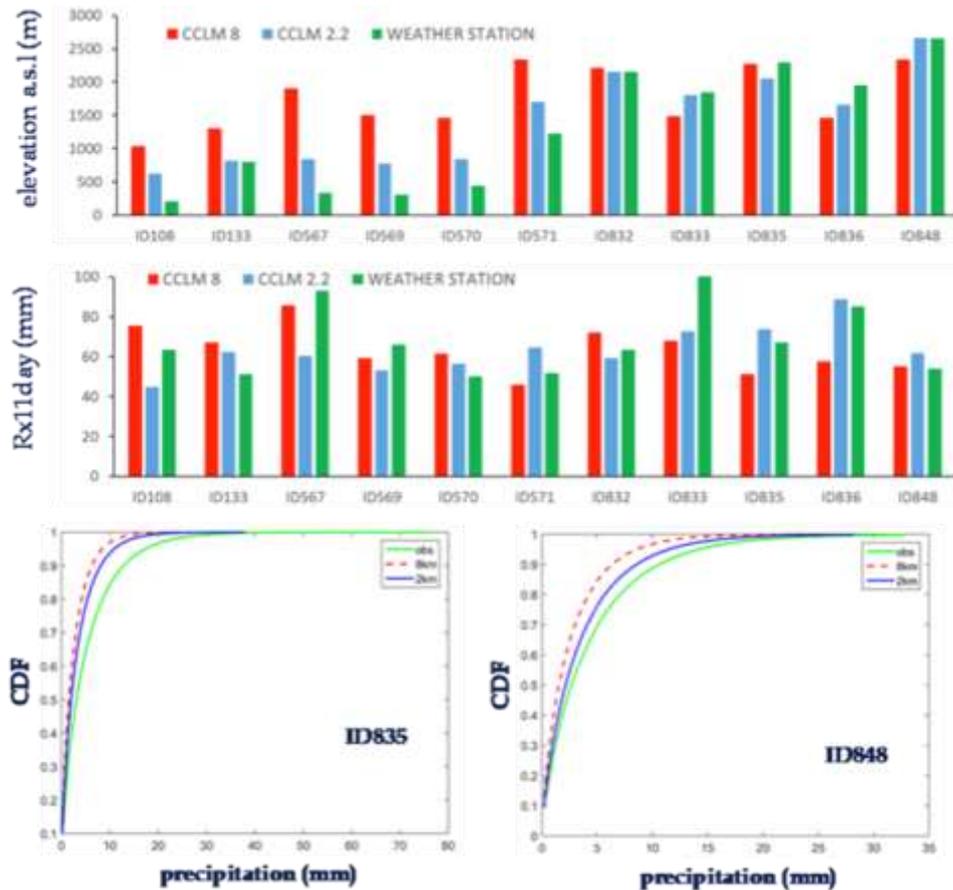

Figure 18. Comparison of elevation and Rx1day between CCLM 8, CCLM 2.2 and data provided by Local Weather Station (1995-2010); gamma distribution for ID835 and ID848.

Overall, in terms of orography, CCLM 2.2 returns a better agreement with local station position compared to CCLM 8 especially for lower altitudes. This improves the accuracy of such a simulation in reproducing precipitation patterns as reflected by the local analysis of Rx1day. Table 4 reports the bias obtained for all the local points. In terms of absolute value, CCLM 2.2 provides a gain for the majority of the cases.

The Gamma distributions in Figure 18 suggest a better capability of CCLM 2.2 in reproducing sub-daily precipitation dynamics. In this case, the higher resolution, in fact, captures better the precipitation patterns.

So far, we have discussed the models' capability to reproduce the main features of the Alpine climate and the possible impacts of climate horizontal resolution on the performance of the simulation in reproducing some basic statistical features of a set of indicators related to intense

precipitation occurrences. In the following Section, an evaluation of the climate change as projected with high–resolution models in the Alpine area will be presented and discussed.

ID	CCLM 8	CCLM 2.2	ID	CCLM 8	CCLM 2.2
108	55%	-13%	832	38%	37%
133	101%	39%	833	-37%	-35%
567	34%	-26%	835	34%	55%
569	22%	-18%	836	-9%	-8%
570	74%	2%	848	54%	90%
571	33%	50%			

Table 4. *Local Weather Station Rx1day bias for CCLM 8 and CCLM 2.2; the minimum absolute value for each point is reported in red.*

13.3.3 Climate change projected in the Alpine region

Mountainous areas cover more than half of the territory of the Italian Peninsula. This section provides an overview of the climate change signal on Italian mountain areas, with a special focus on the Alpine region.

Mean Temperature	Tmean	(°C)
Cumulative winter precipitation (December-January-February)	WP	(mm)
Cumulative summer precipitation (June-July-August)	SP	(mm)
95th percentile of precipitation	R95p	(mm)

Table 5. *ETCCDI indicators considered in the analysis.*

The basic features of the observed climate are discussed using the E-OBS (Haylock et al., 2008) dataset, an observed European daily gridded dataset, with a resolution of 0.25° (about 28 km) for temperature and precipitation, covering the reference period 1981-2010.

For the possible future climate conditions, the projections obtained from a dynamical downscaling of scenario simulations performed with the GCM CMCC-CM (Scoccimarro et al., 2011). The downscaling has been performed with horizontal resolution 0.0715° (about 8 km) through an optimized configuration of the RCM COSMO-CLM (Rockel et al., 2008), implemented with a domain centred over the Italian peninsula (Bucchignani et al., 2015). Two RCPs, namely RCP4.5 and RCP8.5, are adopted to estimate future concentration gases. As a reference climate to contrast the future projected changes, current climate simulation from 1981 to 2010 have been considered, performed using the 20C3M IPCC dataset GHG-A-CAG concentrations as historical radiative forcing.

The outputs of both reference climate and scenario simulations have been analysed considering indicators among those proposed by ETCCDI (see Section 13.3.1 and Table 5).

Specifically, Tmean, WP and SP are considered to point out the average climate characteristics in terms of temperature and cumulative precipitation while R95p is selected to describe the precipitation extremes.

For the current climate simulation (1981-2010), the analysis returns in the Alpine area the minimum average temperature value (5.7 °C); winter precipitation is around 143 mm, while summer precipitation is highly significant (286 mm). Moving towards the Prealps and the northern Apennines, the area appears to be characterized by intermediate values in terms of cumulative

winter (187 mm) and summer (169 mm) precipitation and high values, compared to other areas, for extreme precipitation phenomena (28 mm). Finally, the central-southern Apennines and some limited areas of north-western Italy show reduced summer precipitation (76 mm), although winter precipitation shows medium-high values (182 mm). Extreme rainfall events are 19 mm.

For the future projections, the period 2021–2050 has been considered and contrasted with the reference period (1981–2010). Figure 19 and Figure 20 show the difference between projections and reference climate, of Tmean (Figure 19a and 19b), WP (Figure 19c and 19d), SP (Figure 19e and 19f) and R95p (Figure 20a and 20b), for both RCPs (left: RCP4.5; right: RCP8.5) over the Italian domain.
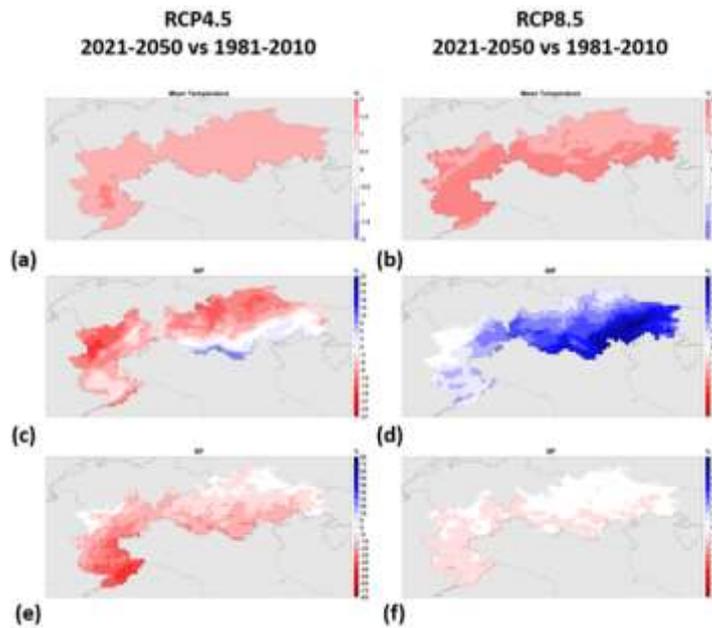

Figure 19. *Tmean (panel a and b), WP (panel c and d) and SP (panel e and f) difference (2021–2050 mean minus 1981–2010 mean) for a RCP4.5 (panel a) and a RCP8.5 (panel b) over the Alpine domain.*

For Temperature mean (Figure 19a and 19b), both RCPs produce warmer conditions, which in the RCP8.5 scenario is more pronounced in the southern flank. When WP is considered (Figure 19c and 19d), the two scenarios, produce a quite remarkably different response. Specifically, a reduction is projected under the RCP4.5 scenario over most of the Alps and especially in the north–western and central sectors, with a reduced WP ranging from -10 to -20 %. While. In contrast, a substantial increment is projected under RCP8.5, especially in the central–eastern sector, with values up to about +30%.
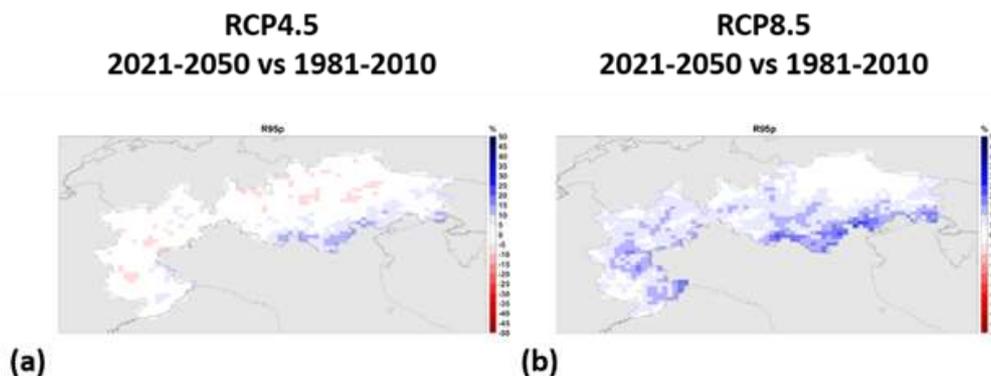

Figure 20. *Extreme precipitation events (R95p) difference (2021–2050 mean minus 1981–2010 mean) for a RCP4.5 (panel a) and a RCP8.5 (panel b) over the Alps.*

Finally, considering the cumulative summer precipitation (SP, Figure 19e and 19f), similar patterns are obtained for both scenarios, with a more pronounced reduction in the south-western Alpine sector, more evident for RCP4.5 than RCP8.5. In the central and eastern part of the Alpine region the projected change of SP is small, particularly in the RCP8.5 scenario.

Figure 20 shows the projected change of R95p for RCP4.5 (Figure 20a) and RCP8.5 (Figure 20b). In both cases, an increase is projected in the south-eastern sector, clearly more pronounced in the RCP8.5 scenario, which shows a projected increase up to +20 / +30 %.

These results obtained for the projected changed over the Alpine region are substantially in line with those reported in literature. For example, Gobiet et al (2014) stated that in the Alpine region, under the A1B emission scenario (similar to the RCP6 in terms of temperature), about 0.25 °C warming per decade until the mid of the 21st century and accelerated 0.36 °C warming per decade in the second half of the century is expected. Warming will probably be associated with changes in the seasonality of precipitation, global radiation, and relative humidity, and more intense precipitation extremes and flooding potential in the colder part of the year. The conditions of currently record breaking warm or hot winter or summer seasons, respectively, may become normal at the end of the 21st century, and there is indication for droughts to become more severe in the future. Snow cover is expected to drastically decrease below 1500–2000 m and natural hazards related to glacier and permafrost retreat are expected to become more frequent. On the same domain, Smiatek et al (2016) investigated the Greater Alpine Region (GAR) considering RCM simulations performed within the Coordinated Downscaling Experiment initiative (CORDEX) at 0.11° resolution (about 12 km) with boundary forcing from five different Coupled Model Intercomparison Project Phase 5 (CMIP 5). The Authors showed that temperature calculations for 2071–2100 against 1971-2000 area return an Ensemble Mean (EM) increases in the seasonal Tmean of 2.5°C in fall and winter, 2.4°C in summer, and 1.9°C in spring. In the same area, precipitation is simulated to increase up to 12.3% in winter and 5.7% in spring. Only minor changes of the ensemble mean are predicted with +2.3% in fall and −1.7% in summer.

References

Allan R. P., Soden B. J., 2008. Atmospheric warming and the amplification of precipitation extremes. Science 321:1481–1484. doi:10.1126/science.1160787.

Ban N., Schmidli J., Schär C., 2014. Evaluation of the convection-resolving regional climate modeling approach in decade-long simulations. Journal of Geophysical Research: Atmospheres 119: 7889–7907. doi: 10.1002/2014JD021478.

Bolvin D. T., Adler R. F., Huffman G. J., Nelkin E. J., Poutiainen J. P., 2009. Comparison of GPCP monthly and daily precipitation estimateswith high-latitude gauge observations. J. Appl. Meteorol. Climatol. 48:1843–1857. doi:10.1175/2009JAMC2147.1.

Bucchignani E., Mercogliano P., Manzi M., Montesarchio M., Rillo V., 2013. Assessment of ERA-Interim Driven Simulation Over Italy with COSMO-CLM. CMCC Research Paper No. 183. Available at SSRN: https://ssrn.com/abstract=2490939 or http://dx.doi.org/10.2139/ssrn.2490939.

Bucchignani E., Montesarchio M., Zollo A. L., Mercogliano P., 2015. High resolution climate simulations with COSMO-CLM over Italy: performance evaluation and climate projections for the 21st century, submitted to Inter-national Journal of Climatology.

Buzzi A. and Speranza A., 1986. A Theory of Deep Cyclogenesis in the Lee of the Alps. Part II: Effects of Finite Topographic Slope and Height. J. Atmos. Sci., 43:2826–2837, https://doi.org/10.1175/1520-0469(1986)043<2826:ATODCI>2.0.CO;2.

Cavicchia L., Scoccimarro E., Gualdi S., Marson P., Ahrens B., Berthou S., Conte D., Dell'Aquila A., Drobinski P., Djurdjevic V., Dubois C., Gallardo C., Li L., Oddo P., Sanna A., Torma C., 2018. Mediterranean extreme precipitation: a multi‑model assessment. Clim. Dyn., 51:901–913, DOI 10.1007/s00382-016-3245-x.

Chou C., Neelin J. D., Chen C., Tu J., 2009. Evaluating the 'rich-getricher' mechanism in tropical precipitation change under global warming. J. Clim. 22:1982–2005. doi:10.1175/2008JCLI2471.1.

Coppola E., Giorgi F., 2010. An assessment of temperature and precipitation change projections over Italy from recent global and regional climate model simulations. Int. J. Climatol. 30:11–32, doi: 10.1002/joc.1867.

Dee D., Uppala S., Simmons A., Berrisford P., Poli P., Kobayashi S., Andrae U., Balmaseda M., Balsamo G., Bauer P., Bechtold P., Beljaars A., van de Berg L., Bidlot J., Bormann N., Delsol C., Dragani R., Fuentes M., Geer A., Haim-berger L., Healy S., Hersbach H., Holm E., Isaksen L., Kallberg P., Kohler M., Matricardi M., McNally A., Monge-Sanz B., Morcrette J., Park B., Peubey C., de Rosnay P., Tavolato C., Thepaut J., Vitart F., 2011. The era-interim reanalysis: configuration and performance of the data assimilation system. Q. J. R. Meteorol. Soc. 137:553–597, doi: 10.1002/qj.828.

Dell'Aquila A., Calmanti S., Ruti P. M., Struglia M. V., Pisacane G., Adriana C., Sannino G., 2012. Impacts of seasonal cycle fluctuations over the Euro-Mediterranean area using a Regional Earth System model. Climate Research, 2, 135.

Dell'Aquila A., Mariotti A., Bastin S., Calmanti S., Cavicchia L., Deque M., Djurdjevic V., Dominguez M., Gaertner M., Gualdi S., 2018. Evaluation of simulated decadal variations over the Euro-Mediterranean region from ENSEMBLES to Med-CORDEX. Clim. Dyn, 51:857–876. https://doi.org/10.1007/s00382-016-3143-2.

Feser F., Rockel B., von Storch H., Winterfeldt J., Zahn M., 2011. Regional Climate Models Add Value to Global Model Data: A Review and Selected Examples. Bull. Amer. Meteor. Soc., 92:1181–1192. doi: http://dx.doi.org/10.1175/2011BAMS3061.1.

Giorgi F., 2006. Climate change hot-spots. Geophys. Res. Lett. 33: L08707, doi: 10.1029/2006GL025734.

Giorgi and P. Lionello, 2008 Climate change projections for the Mediterranean region. Global Planet. Change, 63:90–104.

Giorgi F., Bi X., 2009. Time of emergence (TOE) of GHG-forced precipitation change hot-spots. Geophys. Res. Lett. 36:L06709. doi:10.1029/2009GL037593.

Gobiet A., S. Kotlarski, M. Beniston, G. Heinrich, J. Rajczak, M. Stoffel, 2014: 21st century climate change in the European Alps—A review. Sci. Total Environ., 493:1138-1151.

Gualdi S., Somot S., Li L., Artale V., Adani M., Bellucci A., Braun A., Calmanti S., Carillo A., Dell'Aquila A., Déqué M., Dubois C., Elizalde A., Harzallah A., Jacob D., L'Hévéder B., May W., Oddo P., Ruti P., Sanna A., Sannino G., Scoccimarro E., Sevault F., Navarra A., 2013. The CIRCE simulations: a

new set of regional climate change projections performed with a realistic representation of the Mediterranean Sea. Bull. Amer. Meteo. Soc., 94:65–81, DOI: 10.1175/BAMS-D-11-00136.1.

Haylock M. R., Hofstra N., Klein Tank A. M. G., Klok E. J., Jones P. D., New M., 2008. A European daily high-resolution gridded data set of surface temperature and precipitation for 1950–2006. J. Geophys. Res. 113: D20119, doi: 10.1029/2008JD010201.

Harris I., Jones P. D., Osborn T. J., Lister D. H., 2013. Updated high-resolution grids of monthly climatic observations – the CRU TS3.10 Dataset. Int. J. Clim., 34:623–642.

Iorio J., Duffy P., Govindasamy B., Thompson S., Khairoutdinov M., Randall D. 2004. Effects of model resolution and subgrid-scale physics on the simulation of precipitation in the continental United States. Clim. Dyn. 23:243–258.

IPCC, 2007. Climate Change 2007: The Physical Science Basis. Contribution of Working Group I to the Fourth Assessment Report of the Intergovernmental Panel on Climate Change [Solomon, S., D. Qin, M. Manning, Z. Chen, M. Marquis, K.B. Averyt, M.Tignor and H.L. Miller (eds.)]. Cambridge University Press, Cambridge, United Kingdom and New York, NY, USA.

IPCC, 2012. Managing the Risks of Extreme Events and Disasters to Advance Climate Change Adaptation. A Spe-cial Report of Working Groups I and II of the Intergovernmental Panel on Climate Change, [Field CB, Barros V, Stocker TF, Qin D, Dokken DJ, Ebi KL, Mastrandrea MD, Mach KJ, Plattner GK, Allen SK, Tignor M, Midgley PM (eds.)]. Cambridge University Press, Cambridge, UK, and New York, NY, USA, 2012.

IPCC, 2013. Climate Change 2013: The Physical Science Basis. Contribution of Working Group I to the Fifth Assessment Report of the Intergovernmental Panel on Climate Change [Stocker, T.F., D. Qin, G.K. Plattner, M. Tignor, S.K. Allen, J. Boschung, A. Nauels, Y. Xia, V. Bex and P.M. Midgley (eds.)]. Cambridge University Press, Cambridge, United Kingdom and New York, NY, USA, 1535 pp, doi:10.1017/CBO9781107415324

Isotta F. A., Frei C., Weilguni V., Tadic M. P., Lassègues P., Rudolf B., Pavan´ V., Cacciamani C., Antolini G., Ratto S. M., Munari M., Micheletti S., Bonati V., Lussana C., Ronchi C., Panettieri E., Marigo G., Vertacnik G., 2014. The climate of daily precipitation in the Alps: development and analysis of a high-resolution grid dataset from pan-Alpine rain-gauge data. Int. J. Climatol. 34(5):1657–1675, doi: 10.1002/joc.3794.

Jacob D., Petersen J., Eggert B., Alias A., Christensen O. B., Bouwer L. M., Braun A., Colette A., Déqué M., Georgievski G., Georgopoulou E., Gobiet A., Menut L., Nikulin G., Haensler A., Hempelmann N., Jones C., Keuler K., Kovats S., Kröner N., Kotlarski S., Kriegsmann A., Martin E., van Meijgaard E., Moseley C., Pfeifer S., Preuschmann S., Radermacher C., Radtke K., Rechid D., Rounsevell M., Samuelsson P., Somot S., Soussana J. F., Teichmann C., Valentini R., Vautard R., Weber B., Yiou P., 2014. EURO-CORDEX: new high-resolution climate change projections for European impact research. Reg. Environ. Change 14:563–578, doi: 10.1007/s10113-013-0499-2.

Karl T. R., Nicholls N., Ghazi A., 1999. CLIVAR/GCOS/WMO workshop on indices and indicators for climate extremes: Workshop summary. Climatic Change, 42:3-7.

Kopparla P., Fischer E. M., Hannay C., Knutti R. 2013. Improved simulation of extreme precipitation in a high-resolution atmosphere model. Geophys. Res. Lett. 40:5803–5808.

Mariotti A., Struglia M. V., Zeng N., Lau K. M., 2002°. The hydrological cycle in the Mediterranean region and implications for the water budget of the Mediterranean Sea. J. Climate, 15:1674–1690.

Mariotti A., Zeng N., Lau K. M., 2002b. Euro-Mediterranean rainfall and ENSO—a seasonally varying relationship. Geophys. Res. Lett., 29:591–594.

Mariotti A., Pan Y., Zeng N., Alessandri A., 2015. Long-term climate change in the Mediterranean region in the midst of decadal variability. Clim. Dyna., 44:1437–1456.

Meehl G. A. and Bony S., 2011. Introduction to CMIP5. Clivar Exchanges 16:4-5.

Montesarchio M., Zollo A., Bucchignani E., Mercogliano P., Castellari S., 2014. Performance evaluation of high-resolution regional climate simulations in the Alpine space and analysis of extreme events. J. Geophys. Res. Atmos. 119: 3222–3237, doi: 10.1002/2013JD021105.

Perkins S. E., Pitman A. J., Holbrook N. J., McAneney J., 2007. Evaluation of theAR4 climate models' simulated daily maximum temperature, minimum temperature, and precipitation over Australia using probability density functions. J. Clim. 20:4356–4376.

Prein A. F., Langhans W., Fosser G., Ferrone A., Ban N., Goergen, K., Keller M., Tölle M., Gutjahr O., Feser F., Brisson E., Kollet S., Schmidli J., van Lipzig N. P. M., Leung R., 2015. A review on re-gional convection-permitting climate modeling: Demonstrations, prospects, and challenges. Reviews of Geophys-ics, 53(2):323–361. https://doi.org/10.1002/2014RG000475.

Rajczak J., Schär C., 2017. Projections of future precipitation extremes over Europe: A multimodel assess-ment of climate simulations. J. Geophys. Res.-Atmos., 122:10773–10800, https://doi.org/10.1002/2017JD027176.

Riahi K., Rao S., Krey V., Cho C., Chirkov V., Fischer G., Kindermann G., Nakicenovic N., Rafaj P., 2011. RCP 8.5—a scenario of comparatively high greenhouse gas emissions. Clim. Chang. 109:33–57. doi:10.1007/s10584-011-0149-y.

Rockel B., Will A., Hense A., 2008. The regional climate model COSMO-CLM (CCLM). Meteorol. Z. 17(4):347–348, doi: 10.1127/ 0941-2948/2008/0309.

Ruti P. M., S. Somot, F. Giorgi, C. Dubois, E. Flaounas, Obermann A., Dell'Aquila A., Pisacane G., Harzallah A., Lombardi E., Ahrens B., Akhtar N., Alias A., Arsouze T., Aznar R., Bastin S., Bartholy J., Béranger K., Beuvier J., Bouffies-Cloché S., Brauch J., Cabos W., Calmanti S., Calvet J. –C., Carillo A., Conte D., Coppola E., Djurdjevic V., Drobinski P., Elizalde-Arellano A., Gaertner M., Galàn P., Gallardo C., Gualdi S., Goncalves M., Jorba O., Jordà G., L'Heveder B., Lebeaupin-Brossier C., Li L., Liguori G., Lionello P., Maciàs D., Nabat P., Önol B., Raikovic B., Ramage K., Sevault F., Sannino G., Struglia V., Sanna A., Torma C., Vervatis V., 2016. MED-CORDEX initiative for Mediterranean climate studies. Bull. Amer. Meteo. Soc., 97:1187-1208.

Sanna A., Lionello P., Gualdi S., 2013. Coupled atmosphere ocean climate model simulations in the Mediterranean region: effect of a high-resolution marine model on cyclones and precipitation. Nat. Hazards Earth Sys. Sci., 13:1567-1577   DOI: 10.5194/nhess-13-1567–2013.

Scoccimarro E., Gualdi S., Bellucci A., Sanna A., Fogli P., Manzini E., Vichi M., Oddo P., Navarra A., 2011. Effects of tropical cyclones on ocean heat transport in a high resolution coupled general circulation model. J. Clim. 24:4368–4384, doi: 10.1175/2011JCLI4104.1.

Scoccimarro E., Gualdi S., Bellucci A., Zampieri M., Navarra A., 2013. Heavy precipitation events in a warmer climate: results from CMIP5 models. J. Climate, 26:7902–7911.

Scoccimarro E., Gualdi S., Bellucci A., Zampieri M., Navarra A., 2016. Heavy precipitation events over the Euro-Mediterranean region in a warmer climate: results from CMIP5 models. Regional Environmental Change, 16:595-602.

Soares P. M. M., Cardoso R. M., Miranda P. M. A., Viterbo P., Belo-Pereira M., 2012. Assessment of the ENSEMBLES re-gional climate models in the representation of precipitation variability and extremes over Portugal. J. Geophys. Res. Atmos. 117, D07114, doi: 10.1029/ 2011JD016768.

Smiatek G., Kunstmann H., Senatore A., 2016. EURO-CORDEX regional climate model analysis for the Greater Alpine Region: Performance and expected future change. J. Geophys. Res., 121:7710-7728. https://doi.org/10.1002/2015JD024727.

Taylor K. E., Stouffer R. J., Meehl G. A., 2012. An overview of CMIP5 and the experiment design. Bull. Am. Meteorol. Soc. 93:485–498, doi: 10.1175/BAMS-D-11-00094.1.

Tebaldi C., Hayhoe K., Arblaster M. J., Meehl G. A., 2006. Going to the extremes. An intercomparison of model-simulated historical and future changes in extreme events. Clim. Chang. 79:185–211. doi:10.1007/s10584-006-9051-4.

Van Der Linden P., Mitchell J., 2009. Ensembles: Climate Change and Its Impacts – Summary of Research and Re-sults from the Ensembles Project. Met Office Hadley Centre: Exeter, UK, 1–160.

Vautard R., Gobiet A., Jacob D., Belda M., Colette A., Déqué M., Fernández J., Garcia-Díez M., Goergen K., Güttler I., Halenka T., Karacostas T., Katragkou E., Keuler K., Kotlarski S., Mayer S., Van Meijgaard E, Nikulin G, Patarˇciˊc M, Scinocca J, Sobolowski S, Suklitsch M, Teichmann C, Warrach-Sagi K., Wulfmeyer V., Yiou P., 2013. The simulation of European heat waves from an ensemble of regional climate models within the EURO-CORDEX pro-ject. Clim. Dyn. 41:2555–2575, doi: 10.1007/s00382-013-1714-z.

Wulfmeyer V., Behrendt A., Kottmeier C., Corsmeier U., Barthlott C., Craig G. C., Hagen M., Althausen D., Aoshima F., Arpagaus M., Bauer H. S., Bennett L., Blyth A., Brandau C., Champollion C., Crewell S., Dick G., Di Girolamo P., Dorn-inger M., Dufournet Y., Eigenmann R., Engelmann R., Flamant C., Foken T., Gorgas T., Grzeschik M., Handwerker J., Hauck C., Höller H., Junkermann W., Kalthoff N., Kiemle C., Klink S., König M., Krauss L., Long C. N., Madonna F., Mobbs S., Neininger B., Pal S., Peters G., Pigeon G., Richard E., Rotach M. W., Russchenberg H., Schwitalla T., Smith V., Steinacker R., Trentmann J., Turner D. D., van Baelen J., Vogt S., Volkert H., Weckwerth T., Wernli H., Wieser A., Wirth M., 2011. The convective and orographically-induced precipitation study (COPS): the scientific strategy, the field phase, and research highlights. Q. J. R. Meteorol. Soc. 137:3–30, doi: 10.1002/qj.752.

Zampieri M., Russo S., di Sabatino S., Michetti M., Scoccimarro E., Gualdi S., 2016. Global assessment of heat wave magnitudes from 1901 to 2010 and implications for the river discharge of the Alps. Sci. Total Environ., 571:1330–1339.

Zollo A. L., Rillo V., Bucchignani E., Montesarchio M., Mercogliano P., 2016. Extreme temperature and precipitation events over Italy: Assessment of high-resolution simulations with COSMO-CLM and future scenarios. International Journal of Climatology, 36 (2):987-1004.